

**DEFLECTION OF RIO SALADO TERRACES DUE TO UPLIFT OF THE
SOCORRO MAGMA BODY, SOCORRO, NEW MEXICO**

by

Lisa Majkowski

**Submitted in Partial Fulfillment of the Requirements of the Degree of
Masters of Science in Geology
December 2008**

**Department of Earth and Environmental Science
New Mexico Institute of Mining and Technology
Socorro, New Mexico, USA**

"Vivian and I are conducting a topographical, geological, astronomical, archeological survey."

-Professor Amelia Rumford (David Fisher, *Dr. Who: The Stones of Blood*, 1978)

ABSTRACT

The Socorro magma body is located in central New Mexico along the intersection of the Socorro fracture zone and the Rio Grande rift. High micro-earthquake activity corresponding to the area of the magma body indicates that it is large and currently active. While the depth and extent of the magma body have been fairly well constrained, the age of the magma body is under debate. Evaluation of the surface disruption caused by the magma body can provide clues to the duration of uplift. Specifically, given that the modern rate of vertical deflection can be measured using geodetic techniques, if the amount of deflection of a geomorphic surface above the magma body can be determined, then a minimum age for the initiation of deflection can be estimated by dividing the amount of deflection by the modern rate.

The zone of maximum uplift of the Socorro magma body is localized at the southern end of the Albuquerque basin, near San Acacia, New Mexico. The modern inflation rate of this area of the magma body has been approximated at two to four millimeters per year, based on leveling surveys and INSAR data. There is ephemeral drainage, the Rio Salado, which flows from west to east into the zone of maximum uplift and terminates at the Rio Grande. Rapid and localized uplift of the magma body should deflect the Rio Salado Quaternary terrace surfaces upward from the original longitudinal profile.

Quaternary terraces of the Rio Salado drainage were assessed for uplift deflection. Measurements were made of the terrace elevation above the active channel. Soil development, based on the degree of CaCO_3 accumulation, was used to correlate surfaces and to estimate the relative ages of the terraces. Uplift due to magma inflation should predictably produce vertical displacement of a riverbed and any associated terraces. The modern longitudinal stream and paleostream profiles of a drainage are typically subparallel, thus reflecting the equilibrium state of the drainage over time. However, in a tectonically disturbed region, the longitudinal profiles will deviate from the equilibrium condition with respect to the tectonic source, in this case, the zone of maximum uplift of the magma body. The paleostream longitudinal profiles, as indicated by a distinct sequence of marker terraces, show increasing deflection across the maximum uplift zone.

Although preservation of the Rio Salado terrace surfaces is generally poor, there is one well-developed terrace that can be traced throughout the length of the research area. This marker terrace, Qt6, is distinguished by being the lowest terrace that exhibits Stage III carbonate horizon development and has a profile mass carbonate content ranging from 11.28 to 13.24 g/cm^3 . It is bounded below by a terrace showing weak carbonate horizon development (Stage I) and above by terraces showing greater carbonate accumulation (profile mass carbonate of 15.56 g/cm^3). The Qt6 terrace was identified along the drainage using a series of large soil pits and augered soil-test holes. Elevation of the marker terrace above the active channel increases progressively downstream west to east along the Rio Salado, from 11.66 meters to 17.20 meters near the Rio Grande. The distribution of uplift inferred from the channel deflection is thus consistent with the accepted zone of maximum uplift of the magma body.

ACKNOWLEDGEMENTS

I am indebted to many people who have made the completion of this project possible. I would like to acknowledge and thank my thesis committee, Bruce Harrison, Dave Love and Peter Mozley for their support and guidance regarding this project. Extra thanks go out to Dave Love, who lent me books and equipment and endured long hot days along the Rio Salado measuring terrace elevations, and Peter Mozley, for mapping strategies and very sage advise during the writing phase.

I am especially grateful for the advice and patience of my primary advisor, Bruce Harrison. I thoroughly enjoyed and benefited from the opportunity to work with you. Thank you for treating me as a fellow researcher and for being a true friend.

I would like to thank Penny Boston and Fred Phillips for their invaluable support and constant encouragement.

This project involved a considerable amount of field and lab research. I would like to thank Whitney de Foor, Lee Dalton, Carson Rittel, and Alex Rinehart plus the Geology 403 classes who helped dig and describe soil pits. I would also like to thank

Kalman Oravec and Hugo Gutierrez for a last minute miracle regarding terrace surveying.

Finally, I would like to thank the following people who have shown me much kindness – my mentors, role models and sources of inspiration: Barb Austin, Rob Bowman, Karen Chavez, Michelle Creech-Eakman, Leigh Davidson, Sue Dunston, Julie Ford, Dave Johnson, Lorie Liebrock, Mike Pullin, Snezna Rogelj, Deb Tomanek, and Debbie Wallace.

TABLE OF CONTENTS

	Page
ACKNOWLEDGEMENTS	ii
TABLE OF CONTENTS	iv
LIST OF FIGURES	vi
LIST OF TABLES	viii
LIST OF APPENDICES	xi
INTRODUCTION	1
<i>Geomorphic Setting</i>	8
<i>Previous Work</i>	10
<i>Stream Terrace Correlation and Longitudinal Profiles</i>	15
METHODS	21
<i>Selection of Terrace Surfaces</i>	21
<i>Field Methods</i>	22
<i>Laboratory Analyses</i>	23
RESULTS	25
<i>Upper Reach</i>	28
<i>Silver Creek</i>	34
<i>Loma Pelada</i>	36
<i>Loma Blanca</i>	38

<i>Anticline</i>	41
<i>Rio Salado Longitudinal Profile</i>	43
DISCUSSION	46
<i>Stream Terrace Correlation</i>	46
<i>Estimated age of terraces</i>	47
<i>Estimated duration of uplift</i>	49
<i>Uplift Behavior – Constant or Variable</i>	51
<i>Future Work</i>	54
CONCLUSIONS	56
REFERENCES	58
APPENDICES	61

LIST OF FIGURES

	Page
Figure 1: Map of microearthquake activity in New Mexico and areal extent of Socorro Magma Body	2
Figure 2: Schematic of Socorro magma body microearthquakes and land surface	2
Figure 3: Microearthquake activity concentrated in area of Socorro magma body	3
Figure 4: Uplift rate in mm/year derived from 1992-1999 interferograms	6
Figure 5: Longitudinal profiles in various tectonic settings	7
Figure 6: Study area location map	8
Figure 7A: Leveling survey benchmarks and outline of magma body	11
Figure 7B: Contour map of uplift between 1934 and 1958	11
Figure 8A: Map of 1951 to 1980 leveling survey	12
Figure 8B: N-S uplift profile and topography	12
Figure 9: Profile of Loma Parada surface along Rio Grande River	13
Figure 10: Illustration of different types of terraces	17
Figure 11: Potential issues for terrace correlation	20
Figure 12: Extent of study area of the Rio Salado	25

Figure 13:	Study area sections along the Rio Salado	26
Figure 14:	Upper Reach section of the study area	30
Figure 15:	Qt6 soil from Silver Creek section	32
Figure 16:	Qt7 soil from Loma Pelada section	33
Figure 17:	Silver Creek section of the study area	35
Figure 18:	Loma Pelada section of the study area	37
Figure 19:	Loma Blanca section of the study area	40
Figure 20:	Anticline section of the study area	42
Figure 21:	Longitudinal profile of the Rio Salado	43
Figure 22:	Longitudinal profile of Qt5, Qt6 and Qt7	44

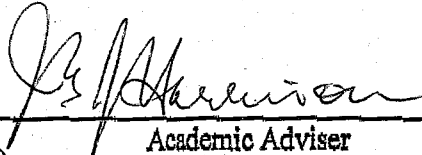
LIST OF TABLES

	Page
Table 1: Terrace elevations above the modern channel	31
Table 2: Profile mass carbonate of Qt5, Qt6 and Qt7 terrace surfaces	31
Table 3: Maximum duration of uplift as determined from Qt6 elevation above modern Rio Salado channel	49
Table 4: Minimum duration of uplift of Qt6 terraces surfaces determined from adjusted Qt6 terrace altitudes	51

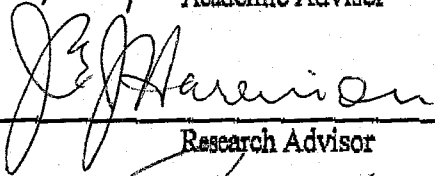
LIST OF APPENDICES

	Page
Appendix A: Elevations of surveyed terraces	61
Appendix B: Soil Descriptions	63
Appendix C: Soil Laboratory Analyses	66

This Thesis is accepted on behalf of the faculty
of the Institute by the following committee:



Academic Adviser



Research Advisor



Committee Member

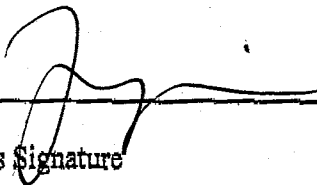


Committee Member

Committee Member

Date

I release this document to New Mexico Institute of Mining and Technology



Students Signature



Date

INTRODUCTION

The Socorro magma body (SMB) (Figure 1) is a large, mid-crustal, sill-shaped magma body located near Socorro, New Mexico (Larsen and Reilinger, 1983; Sanford, 1983; Fialko and Simons, 2001). Seismic reflection data shows the SMB having a horizontal area greater than 2000 km² at a depth of 19-20 km (Hartse and Sanford, 1992; Sheetz and Schlue, 1992; Fialko and Simons, 2001) (Figure 2). Socorro lies along the Rio Grande Rift, and while magmatism is often associated with continent rifts (MacDonald, 1972; Sanford, 1983), detection of the emplacement of large amounts of magma into the crust is uncommon (Sanford, 1983). Study of the SMB provides insight into magmatic geophysics and will lead to a better understanding of crustal intrusion mechanisms (Fialko and Simons, 2001).

Microearthquake activity in the Socorro area is linked to SMB uplift (Figure 1). Seismicity is caused by magma injection into the crust, with epicenter distribution related to radial extension generated by the uplift (Sanford et al., 1983). Additionally, maximum earthquake activity is clustered within zone of maximum surface uplift (Sanford et al., 1983). Average uplift rates for the magma body have been determined by three different studies (Reilinger and Oliver, 1976; Larsen and Reilinger, 1983; Fialko and Simons, 2001) at 1-5 mm per year.

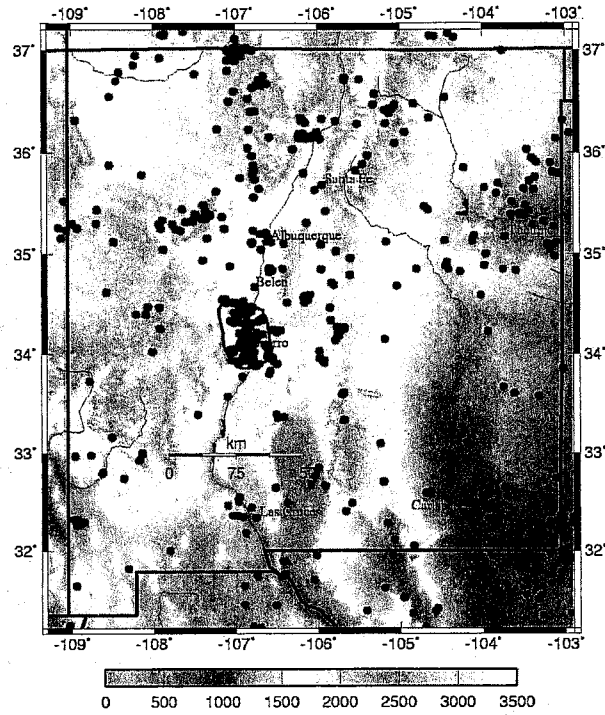


Figure 1: Map of microearthquake activity in New Mexico and areal extent of Socorro Magma Body (Sanford et al., 2006).

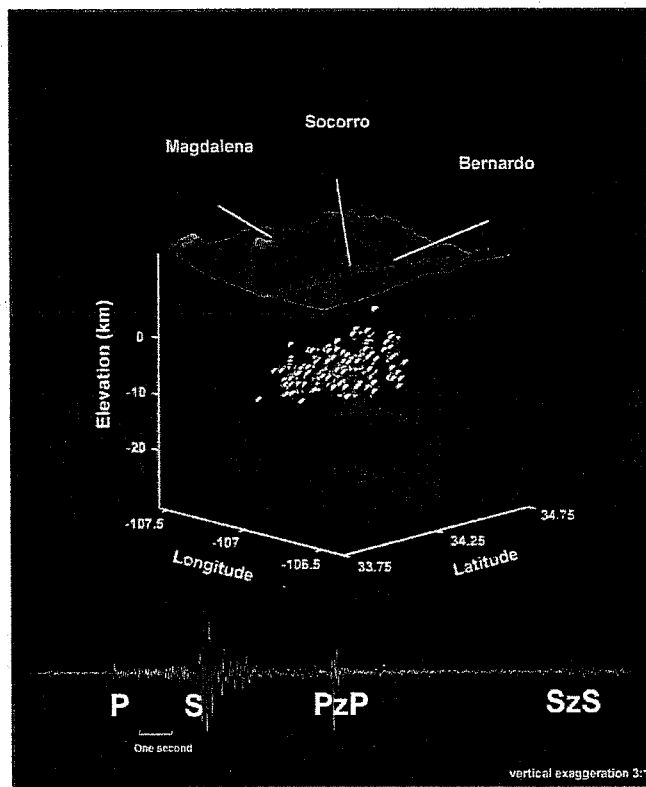


Figure 2: Schematic of Socorro magma body (red), microearthquakes and land surface (Sanford et al., 2006).

Reilinger and Oliver (1976) and then Larsen and Reilinger (1983) developed uplift estimates from repeated, first-order leveling surveys. Both studies calculated maximum total uplift and average uplift relative to a bench mark outside the zone of deformation. Fialko and Simons (2001) compared InSAR satellite interferograms between 1992 and 1999 to derive an average uplift rate for the extent of the SMB (Figure 3).

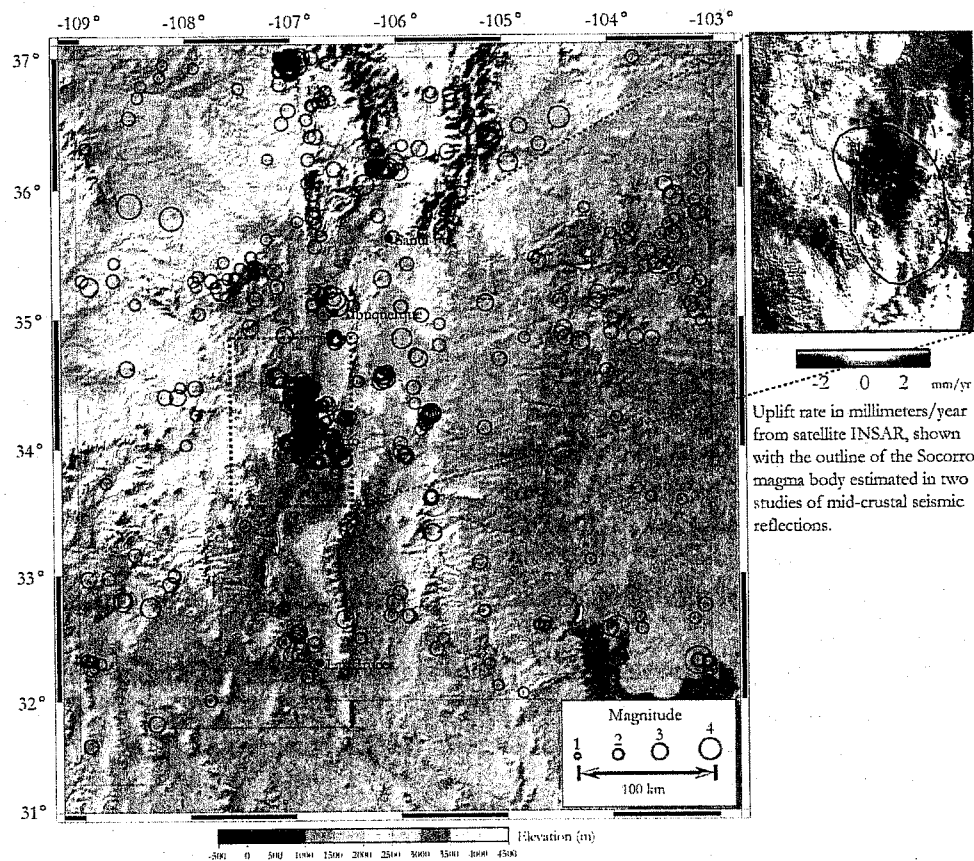


Figure 3: Microearthquake activity concentrated in area of Socorro magma body, insert map shows InSAR image (Sanford et al., 2006)

While the geophysical characteristics of the magma body have been extensively studied, less is known about the timing of the emplacement of the magma body (Larsen et al., 1986; Schlue et al., 1996; Fialko and Simons, 2001). Estimates based on the thickness of the magma body and rates of uplift have provided an approximate age but the

estimates vary by several orders of magnitude. The Larsen et al. (1986) and Schlue et al. (1996) studies propose that the SMB has been steadily inflating since the late Pleistocene, based on the current thickness and volume of the magma body, the total recorded displacement and the seemingly steady rate of inflation (Fialko and Simons, 2001). However, Fialko and Simons (2001), while agreeing with the current inflation rate of the magma body, question the duration of inflation and thickness. They ascertain that the modern thickness of the magma body is insufficient to maintain thermal viability for a duration on the order of 10^4 years. Fialko and Simons (2001) suggest several possibilities: the magma body may be relatively young (on the order of 10^2 years), it may be thicker than estimated, and the surface displacement may be a function of different deformation mechanisms (rather than elastic deformation over the entire area of the magma body). This points to two essential questions: what is the style of uplift and when did uplift begin. Potentially, the magma body could exhibit one of several major behaviors. Inflation could occur at a steady rate, which is consistent with leveling survey data between 1909 and 1979 (Reilinger et al., 1980). Alternatively, uplift could be episodic in response to an inelastic mode of deformation (Fialko and Simons, 2001). Finally, the magma body may "breathe", with differential inflation and subsidence over the extent of the magma body. Two recent studies, Love et al., (2003) and Newman et al., (2004), indicate that inflation of the magma body may exhibit complex behaviors, with counterintuitive tilt responses and rapid transient uplift.

This thesis examines the geomorphic response of the local terrace surfaces to the uplift of the Socorro magma body. Study of the long-term history of the surficial effects

of the uplift should provide clues to the potential inflation mechanism of the Socorro Magma Body and constrain a minimum age of uplift. The Rio Salado drainage and associated terraces cross the zone of maximum uplift of the magma body, allowing for a comparison of the surfaces within and outside of the maximum influence of the SMB (Figure 4).

Terrace surfaces were measured for elevation above the active stream channel. Changes in the terrace elevations above the active channel were studied along the Rio Salado from an area of minimal uplift into the zone of maximum uplift. Proximity to the maximum uplift zone resulted in increasing offset of the terraces above the modern stream channel.

Considering the three major scenarios for uplift, I will compare the longitudinal profile of the modern channel to the longitudinal profile of the paleochannels to indicate the behavior of the uplift. Steady state inflation should produce a continuously increasing curve between the paleostream profiles and the active channel profile into the area of maximum uplift (Figure 5). In this case, offset above the slope of the modern drainage longitudinal profile will be used in conjunction with the uplift rate to constrain the minimum timing of uplift effects on local landscape evolution. Episodic uplift would present similar terrace distributions to steady state inflation and may be difficult to distinguish within the parameters of this study. "Breathing" behavior or differential uplift and subsidence would result in poor terrace preservation, missing or stripped surfaces,

and buried soils. Depending on the frequency of the uplift and subsidence, development of a paleostream profile would be problematic.



Figure 4: Uplift rate in mm/year derived from the Fialko and Simons 1992-1999 interferograms (Love et al., 2003).

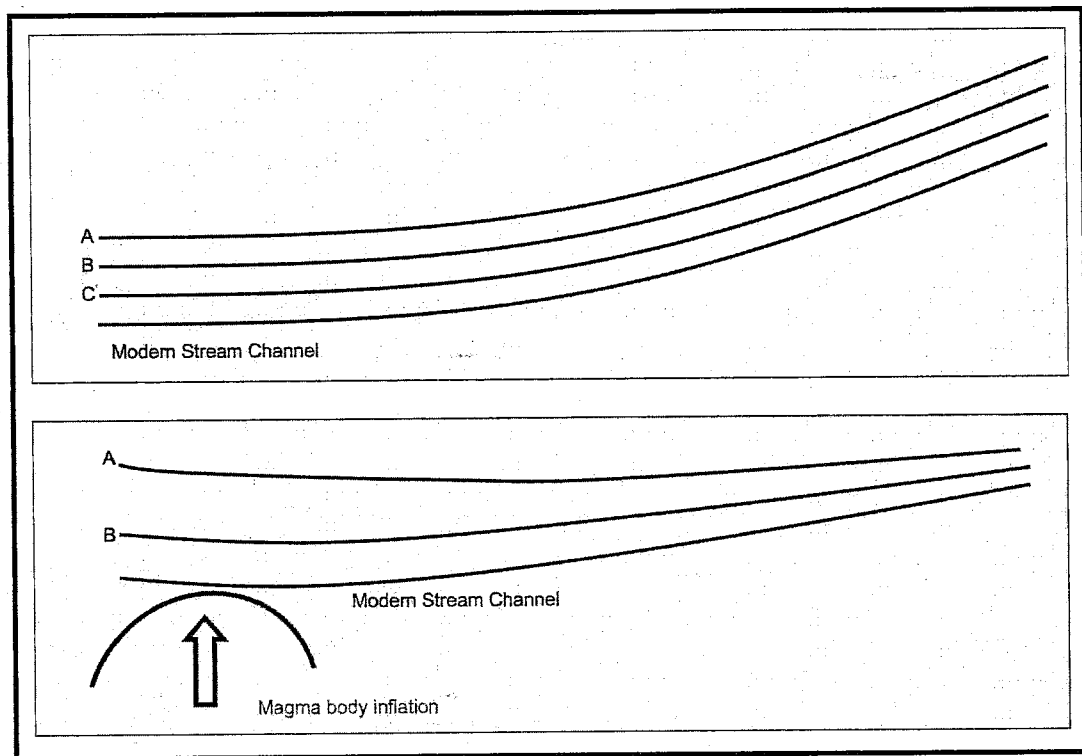


Figure 5: Longitudinal profiles of paleostreams in various tectonic conditions, showing the modern stream channel and sequential paleostream profiles above the modern channel. The top image reflects a sequence of paleostream terraces unaffected by tectonic forcing. The lower image illustrates the deflection of the stream channels due to a zone of localized uplift, such as the Socorro magma body.

Geomorphic Setting

The Rio Salado is located in central New Mexico (Figure 6), approximately 24 kilometers north of Socorro, New Mexico. It originates at the confluence of Alamocito Creek and Gallegos Creek and drains eastward into the Rio Grande. The Rio Salado traverses the La Jencia basin in the west and the southern Albuquerque basin in the east.

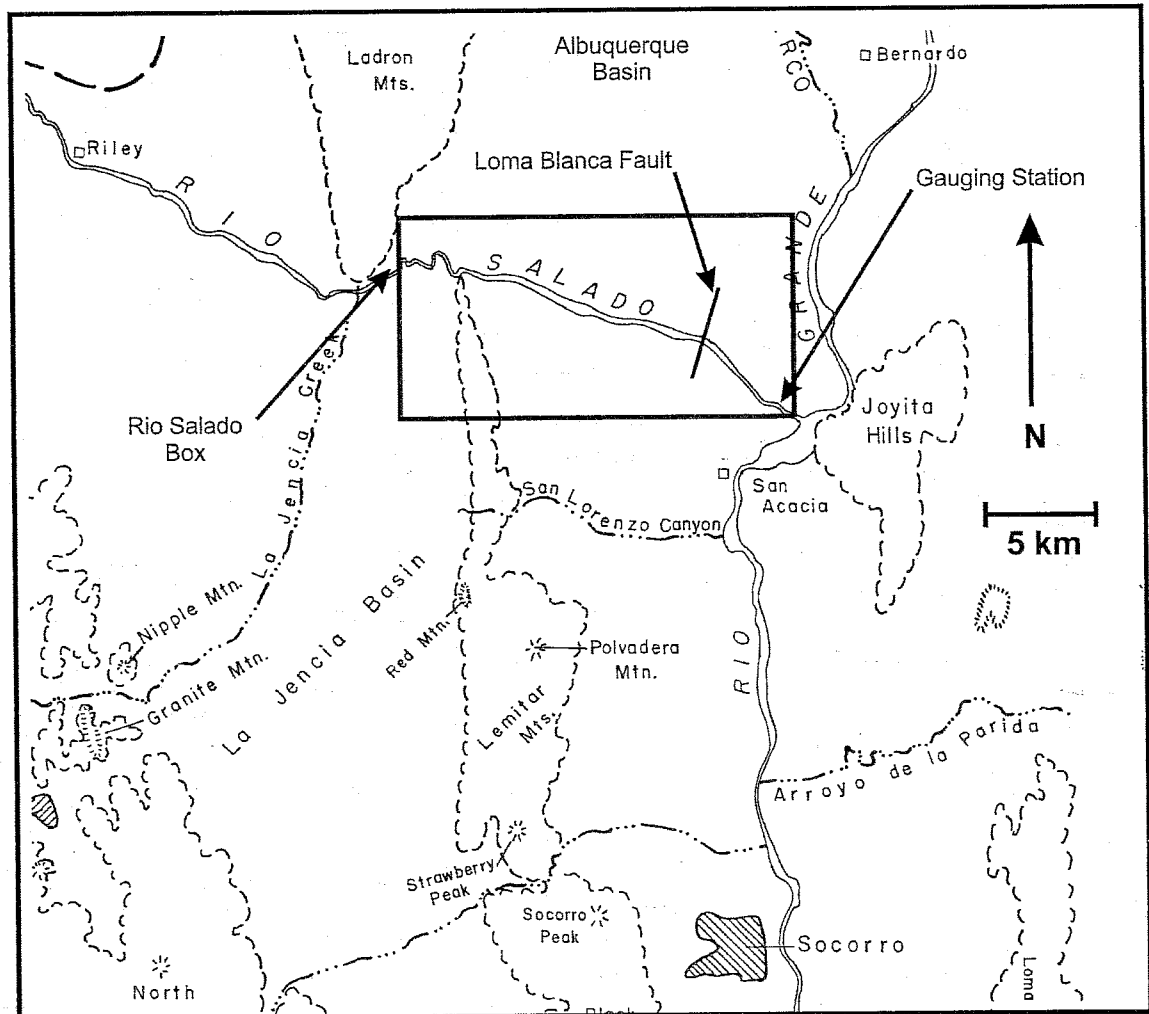


Figure 6: Study area location map (modified from New Mexico Geological Society, 1983).

The Rio Salado is an ephemeral, braided stream with a minimum active channel width within the study area of 48 meters in the upper reaches near the Box and a lower reach width of 250 meters near the gauging station. It is 72 km long with an average gradient of 6.2m/km and an overall drainage area of 3570 km² (Simcox, 1983). Channel deposits range from small boulders to bars of coarse gravels to overbank deposits of fine sand, silt and clays, with an average grain size of 2 to 64 mm (Simcox, 1983).

Rio Salado related geomorphology consists of dissected Quaternary cut and fill strath terraces, piedmont slope alluvial fans and pediments, Holocene eolian dunes and locally sourced colluvium (Machette, 1978). There is significant artificial fill (roadway subgrades, flood levees, canal embankments) occurring in the lower 2.5 km of the drainages (Machette, 1978). The southern margin of the active channel has been bulldozed upstream as far as the Loma Blanca Fault as part of an erosion control program by the Bureau of Reclamation (Gonzales, 2005). Quaternary deposits overlie the Tertiary Popatosa and Sierra Ladrones Formations.

Sand sourced from the Rio Salado forms dunes on the northern margin of the lower reaches of the drainage and east of the Loma Blanca fault (Evans, 1963), although much of the dune field has become stabilized by vegetation over the last twenty years. Quaternary terrace surfaces bordering the Rio Salado (Machette, 1978) are dominated by Chihuahuan Desert Scrub vegetation, including creosotebush, honey mesquite, fourwing saltbush, broom snakeweed, black grama grass, desert holly and blackfoot daisy (Sevilleta LTER Research Sites, 2005).

Previous Work

In order to fully understand the novelty of the approach used in this thesis, it is helpful to review the previous studies of the surface offset due to the Socorro magma body in more detail (Reilinger and Oliver, 1976; Reilinger et al., 1980; Larsen and Reilinger, 1983; Ouchi, 1983; Fialko and Simons, 2001). These studies are in relative agreement on the approximate area of uplift and uplift rates, ranging from one to five millimeters per year.

Reilinger et al. (1980) reported surface uplift corresponding to the spatial boundary of the Socorro magma body, with an estimated uplift rate of 5 mm/yr for the period between 1909 and 1979 (Figure 7). They derived their estimates from first-order leveling studies carried out by the National Geodetic Survey, with a north-south transect running from Albuquerque, New Mexico to El Paso, Texas as well as an east-west transect from Socorro, New Mexico to Magdalena, New Mexico and from Belen, New Mexico to Amarillo, Texas. Reilinger et al. (1980) calculated an average inflation rate for the magma body that is comparable to modern inflation rates in areas of volcanic activity (~ 1 to 2×10^{-2} km³/yr). Further more, the magma body activity must be episodic on a longer time frame based on estimates of post-Pliocene stream bed tilt rates (an order of magnitude less than indicated by modern, geodetic data).

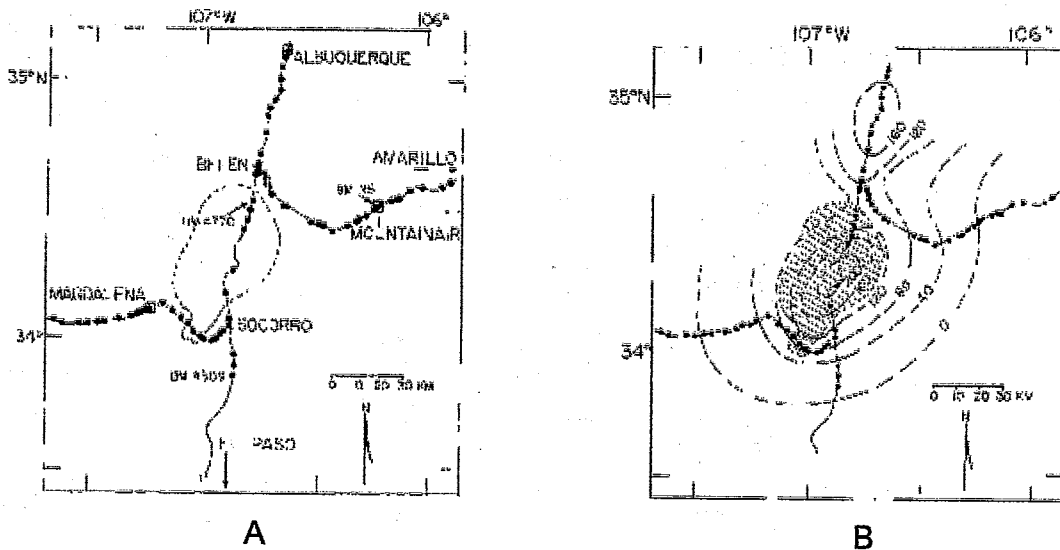
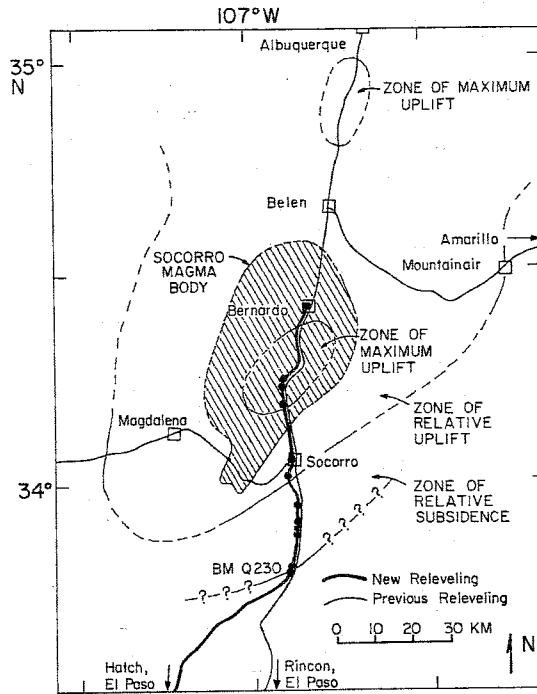
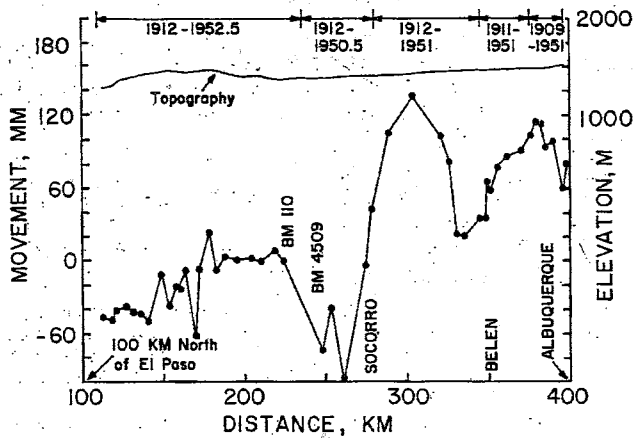
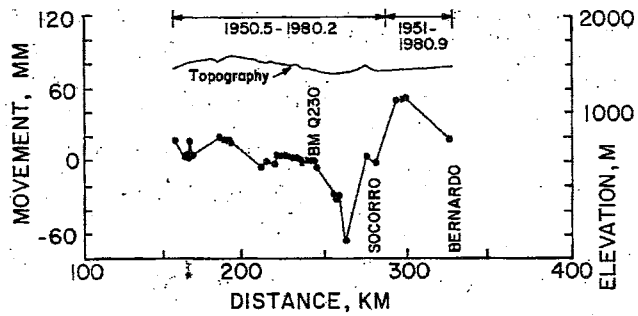


Figure 7: A - Leveling survey benchmarks and outline of magma body; B - Contour map of uplift between 1934 and 1958 (Reilinger et al., 1980).

Larson and Reilinger (1983) refined Reilinger et al.'s earlier work by using new National Geodetic Survey releveling data from 1980 (Figure 8). Crustal movement is calculated from the difference in elevation between a given bench mark and a reference bench mark and then subtracting that difference from the elevation data of the previous leveling study. Larsen and Reilinger noted that there was an area of relative subsidence south of Socorro, New Mexico. They calculated a new uplift rate of 1.8 mm/yr during the period between 1951 and 1980, which coincided with decreased seismic activity for the same period. This work supports the idea that the magma body processes are potentially complex.



(A)



(B)

Figure 8: (A) Map of 1951 to 1980 leveling survey; (B) N-S uplift profile and topography (Larsen and Reilinger, 1983).

Ouchi (1983) studied ancestral Rio Grande terraces within the central area of the uplift between La Joya and San Acacia, New Mexico. He noted that the Loma Parda surface, a set of correlated Pleistocene terraces, showed deformation within the extent of the uplift. Based on the time of incision of the Loma Parda surface by the Rio Grande, Ouchi calculates the uplift rate at 1.8 mm/yr, consistent with the findings of Larsen and Reilinger. Ouchi also offers that convexities apparent in the longitudinal profiles of the Rio Grande between 1917 and 1972 may be due to uplift of the Socorro magma body (Figure 9). Although it is expected that the Rio Grande would maintain equilibrium with the slow uplift by down-cutting, Ouchi suggests that the Rio Grande could not maintain a profile within the zone of uplift because of the high sediment supply contributed by the Rio Puerco and the Rio Salado.

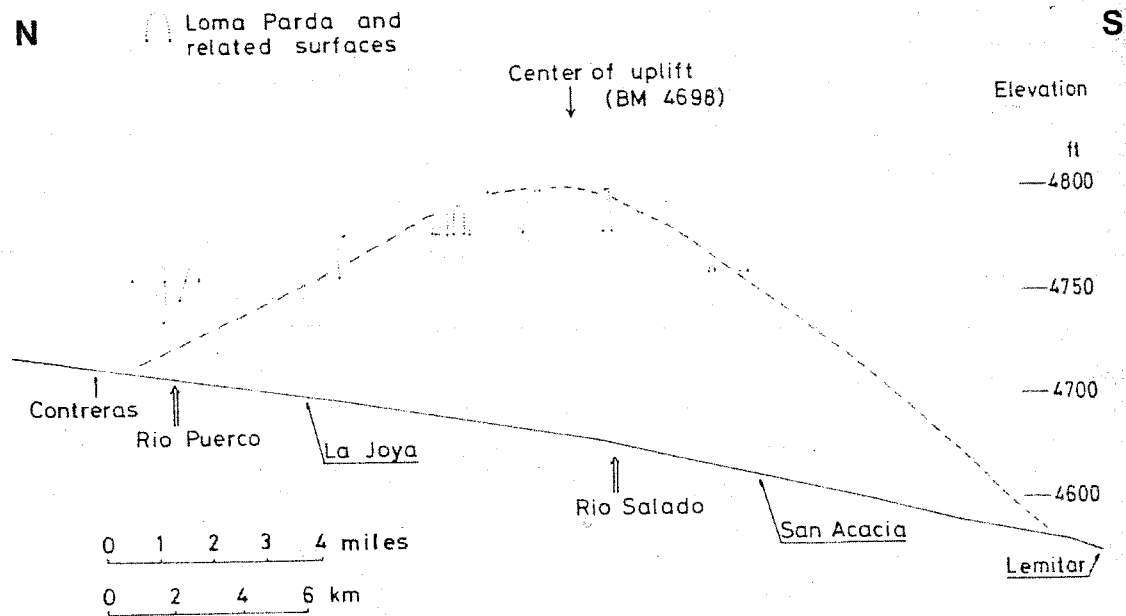


Figure 9: Loma Parda surface within zone of maximum uplift of SMB. Profile of Loma Parda surface along Rio Grande River (Ouchi, 1983).

Fialko and Simons (2001) conducted InSAR (Interferometric synthetic aperture radar) studies of central New Mexico between 1992 and 1999. They outlined the area of maximum uplift of the magma body and further defined its areal extent (Figure 4). Fialko and Simons quote other studies (Bachman and Mehnert, 1978; Ouchi, 1983; Schlue et al., 1996) as stating that the uplift of the Socorro magma body was relatively constant over the last tens of thousands of years. They propose that the duration of uplift rate changes may be on the order of tens of years. Although the InSAR data suggests an average uplift rate of 2-3 mm/yr (consistent with previous studies), Fialko and Simons maintain that thermodynamically, the volume of the magma body (as derived from seismic studies) could not remain active for 100,000 years (as put forward by Ake and Sanford, 1988). They claim that either emplacement of the magma body is relatively recent (hundreds of years) or the magma body is thicker than originally calculated.

Stream Terrace Correlation And Longitudinal Profiles

This study addresses uplift of the Socorro magma body by examining the deflection of Quaternary stream terraces of the Rio Salado drainage with respect to the zone of maximum uplift. The Rio Salado channel crosses the SMB through different zones of uplift (Figure 10). This will allow a comparison of the terrace altitude changes with respect to different uplift rates of zero to four mm per year. The modern Rio Salado channel downcutting may be keeping pace with the surface uplift caused by the magma body, or it too may be deflected upward. The pattern is revealed in the modern longitudinal stream profile. In a system without tectonic perturbations, the paleochannel longitudinal profiles would be sub-parallel to the modern profile (Bull, 1990; Burbank and Anderson, 2001). In a system with tectonic uplift, the paleochannel longitudinal profiles should be deflected by the uplift (Bull, 1990; Burbank and Anderson, 2001) with the greatest uplift in areas with the maximum offset. The longitudinal profile constructed from correlated Quaternary terrace surface elevations above the modern drainage will exhibit a deflection or convexity in slope above the uplift. To determine the minimum age for uplift initiation, the elevation difference between the modern channel and the lowest deflected paleochannel is divided by the uplift rate.

Stream terraces are correlated by relative age, determined by soil development. A characteristic feature of soil development in the semi-arid environment of central New Mexico is the accumulation of pedogenic calcium carbonate (Birkeland, 1984). Although carbonate content does not provide a specific age, the same aged surfaces should show a

similar degree of calcic horizon development and/or amount of calcium carbonate. Soil variability and the influences of deposition and erosion on the same aged terrace surface leads to ambiguities in correlation of surfaces. Surfaces stripped by erosion may be missing the A and B horizons. Surfaces covered by recent deposits will have either no A horizon or a very weakly developed A horizon. By examining the soils of the terraces above and below the terrace of interest, it is possible to constrain the soil development of that terrace and correlate disparate terraces of the same surface.

This study focuses on strath terraces, as they are the best indicators for inception of local, tectonically- driven terrace formation within this system (Bull, 1990; Burbank and Anderson, 2001). Strath terraces are erosional features that form in response to increase stream power (Bull, 1990; Burbank and Anderson, 2001). Tectonic uplift steepens the stream gradient, increasing the stream power (Bull, 1990; Burbank and Anderson, 2001). Strath terraces are easily identifiable – an eroded bedrock terrace covered by no more than three meters of deposits (Birkeland, 1984).

The longitudinal profile of the modern stream channel represents the drainage response to the regional climatic and tectonic forces that regulate the stream power for the drainage. Stream power is “the expenditure of potential energy per unit length of stream” and is proportional to stream slope and discharge (Burbank and Anderson, 2001). The longitudinal profile of a stream channel depicts the elevation of the drainage from its headwaters to its base level, such as where it joins a larger drainage or empties into a basin or an ocean (Burbank and Anderson, 2001). At the regional scale, longitudinal

stream channel profiles should be a smoothly decreasing curve downstream; tectonic perturbations are clearly recognizable (Burbank and Anderson, 2001). The longitudinal profile of a stream channel at base level for a stream that is in equilibrium is time independent (Bull, 1990). There is a balance between the components of discharge and sediment supply.

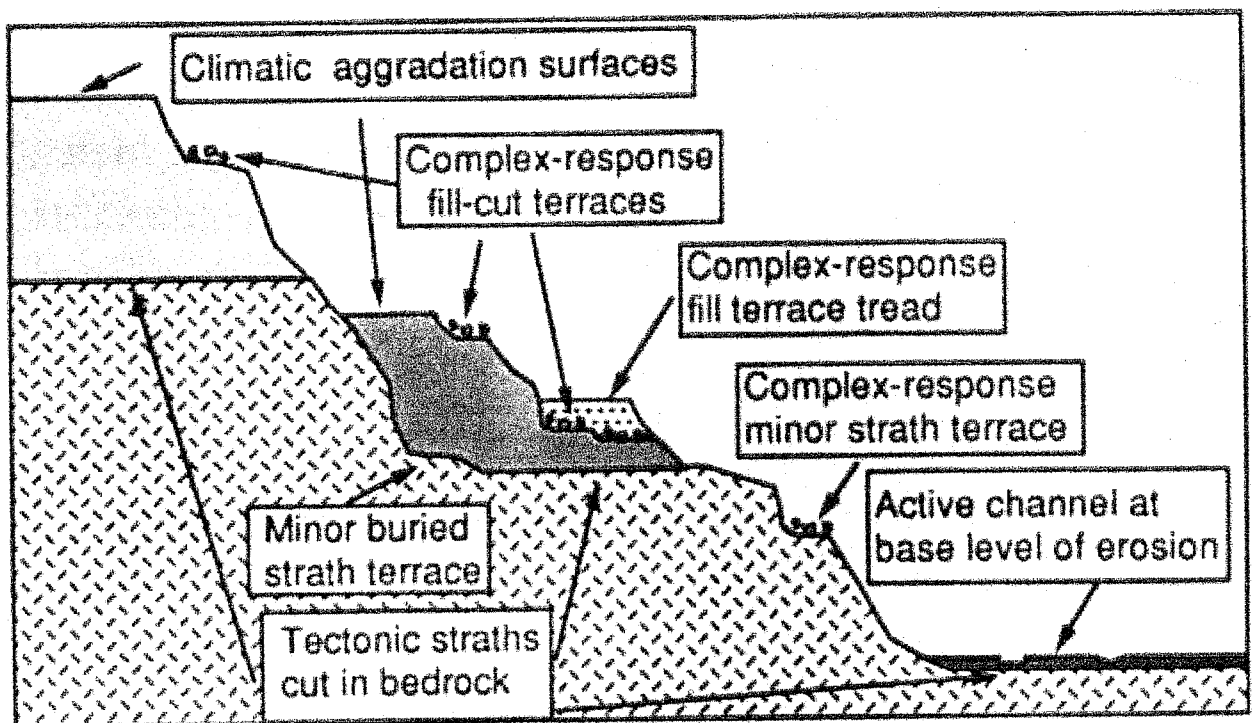


Figure 10: Illustration of different types of terraces (Bull, 1990).

Assuming that the system has been unperturbed by climatic or tectonic events, the longitudinal profiles of age-correlated terraces, representing paleochannel profiles, should be parallel to the longitudinal profile of the active channel. The age of the terrace and its height above the active channel are governed by the base level and are controlled

local uplift rates (Bull, 1990). However, if local tectonic uplift is raising the landscape surface while the active stream continues to maintain erosional equilibrium, the terrace longitudinal profiles should show a deflection above the active channel profile. Further, if the local uplift rate is known, it should be possible to calculate the duration of response to uplift for a specific surface based on its height above the active channel, thereby constraining the age of uplift initiation.

Streams are connected between all parts of the watershed (Bull, 1990), hence the base level of the Rio Salado is ultimately controlled by the Rio Grande. Both drainages flow through the zone of maximum uplift and are affected by local uplift of the magma body. Tectonically-induced downcutting forces stream degradation to maintain a “dynamic equilibrium longitudinal profile at the base level of erosion” (Bull, 1990). As the fundamental tectonic stream surface is the strath terrace, which is formed by lateral erosion of the stream channel (Bull, 1990), this study uses strath terraces to define the paleochannel profile of the Rio Salado. Additionally, the erosional base level cannot be achieved during climatically-driven complex cut and fill response (Bull, 1990), making fill terraces unsuitable.

Relationships between bounding terraces are also used as corroborating evidence for terrace correlation. Terraces are the abandoned flood plain of a channel in response to downcutting by the associated drainage (Bull, 1990). How does this happen? Climatic and tectonic factors change the stream’s power and induce either aggradation or erosion, converting active floodplains into terrace treads (Bull, 1990). Aggradational or fill

terraces occur when climatic forcing increases the amount of bedload available to the system. Erosional or strath terraces occur as a response to tectonically induced downcutting. Complex-response terraces, combinations of fill and strath sequences (Figure 10), form in response to local perturbations of the fluvial system (Bull, 1990). Flights of complex-response terraces form in the vertical space that result from uplift (Bull, 1990).

Correlation of terrace surfaces is essential for developing the paleochannel profiles. Terraces cannot be correlated solely by elevation above active channel (Schumm et al., 1987). The correlation of terrace heights above the active channel assumes that the longitudinal profile has remained constant over time (Burbank and Anderson, 2001). Strath surfaces are controlled by regional and or local tectonic activity; dating is required to correlate surfaces (Figure 11). Additionally, good exposures and dating are crucial to distinguishing static equilibrium complex-response minor strath terraces from tectonically-induced major strath terraces (Bull, 1990).

Difficulties in correlating surfaces along the Rio Salado, include the paucity of appropriate datable materials, lack of extended reaches of continuous terrace surfaces and limited surface preservation. These factors increase the potential for miscorrelation. The preservation of geomorphic markers can degrade with time; however, a distinctive characteristic may allow the correct correlation of remnants (Burbank and Anderson, 2001). The terraces of the southern margin of the Rio Salado possess such a characteristic marker. There are three terraces, Qt5, Qt6 and Qt7, that make up that marker. These

terrace appear along the drainage in a predictable horizontal displacement from one another.

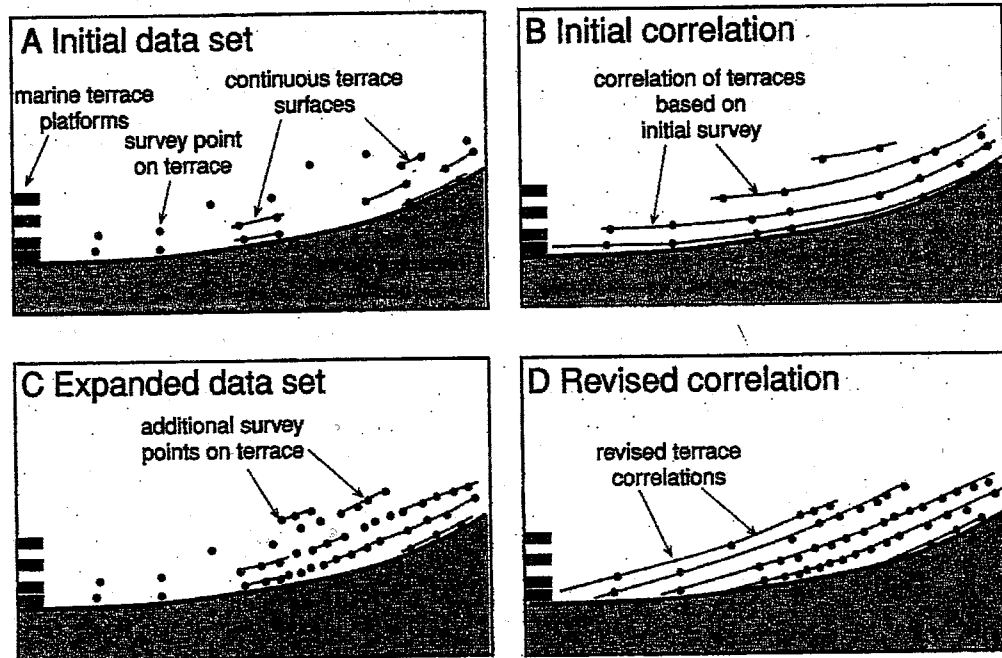


Figure 11: Potential issues when correlating surfaces. As the diagram shows, the correctly correlated surfaces are not sub-parallel to the modern channel. The alignment of the terraces indicates that there was uplift upstream (modified from Burbank and Anderson, 2001).

METHODS

Selection of Terrace Surfaces

This study examined terrace surfaces along 20 kilometers of the Rio Salado drainage, predominantly on the southern side of the channel. The local prevailing wind direction is from the south (Evans, 1963) depositing thick sand sheets on the northern margin of the drainage. In addition to obscuring the terrace surfaces, the sand deposits form a new, younger surface on top of the pre-existing Rio Salado terraces. The result is a similar degree of soil development on different age surfaces (Goldstein, 2001).

Potential terrace surfaces were initially identified by an examination of 1954 aerial photographs of the Rio Salado drainage and then confirmed by field examination. Many terrace surfaces were poorly preserved, especially in the lower reaches of the drainage and at the junction of large tributary channels into the Rio Salado. Early on in the study, it became clear that there was a distinct terrace, Qt6, that could be identified along the length of the study area. This terrace was not laterally continuous along the channel and could be identified through a combination of field methods – soil development, elevation and relationship to other terraces.

Field Methods

Field research focused on identifying terraces that were present within the entire field area, then mapping their extent and elevation as well as soil sampling where appropriate. Terraces were correlated using two key characteristics 1) the presence of well-developed calcic horizon and 2) their spatial relationship to the terraces above and below. There was a very distinct relationship between the Qt5, Qt6 and Qt7 terraces – the elevation differences between the terraces and the degree of soil development on the surfaces aided in maintaining the correlation of the surfaces in areas where terraces might be missing. These three surfaces were utilized as a marker unit for mapping.

Most of the terrace surfaces along the Rio Salado represent remnants of the original surfaces. These surfaces, while not suitable for soil descriptions, the elevations of these points could be used to construct the paleostream profiles. A Dutch-type, combination 7 cm diameter soil auger was used to evaluate the remnant surfaces for depth to carbonate and thus determine if they were part of the marker terraces.

Elevations of the marker terraces above the current channel were measured using a Jacobs staff and Abney level. Elevations were measured from the most recently active channel bottom to the strath (where identifiable) and to the top of the terrace surface. Additional measurements using a total station were made of a flight of terraces located on the north side of the Rio Salado drainage above Silver Creek (Appendix A). The terrace

surfaces were mapped on to USGS 7.5' topographic maps. Field maps were converted into digital format using USGS 7.5' Digital elevation Models (DEMs) and ArcMap 9.1.

Soil pit locations were based on 1) the amount of preservation of the surface, and 2) finding suitable surfaces within each section of the study area. Soil pits were dug in pairs: one on the marker terraces and one on the lower, younger terrace. Additional pits were dug on higher surfaces where suitable conditions were available. Pits ranged from 1 to 2 m³ in size and were located on the flattest part of the surface, away from the influence of colluvial deposition from adjacent terrace risers or hillslopes.deposits. Locations of pits were obtained using a Garmin Rhino GPS.

Soil profiles were described according to section of the NRCS Field Book for Describing and Sampling Soils (NRCS, 2002) and each horizon sampled for laboratory analysis (Appendix B). The soil profiles were digitally photographed with a scale.

Laboratory Analyses

Laboratory analyses of the collected soil samples included particle size distribution analysis (PSDA), bulk density of soil <2mm fraction, and calcium carbonate (CaCO₃) percent, following methods described by Singer and Janitsky (1986) (Appendix C). Samples were run in random order to reduce bias.

Samples were collected for each horizon of each pit. Multiple samples were collected for thick horizons (greater than 30 cm), at a 20 cm interval when possible. Samples were mechanically bulk split and then sieved to separate the <2mm fraction. Fine fractions were then split for individual analyses.

The particle size distribution analysis procedure operates on Stoke's Law, which states that particle settling rate is proportional to particle size and mass (Janitzky, 1986). Most of the samples were determined in the field to have insufficient CaCO_3 content to warrant carbonate digestion pretreatment. Clays contained within the sample were dispersed using a 10% solution of sodium pyrophosphate ($\text{Na}_4\text{P}_2\text{O}_7$). Sand, silt and clay percentages were determined using the pipette method (Day, 1965; Jackson, 1969; Singer and Janitzky, 1986).

Bulk density was determined using the paraffin clod method (Blake, 1965; Singer, 1986). Bulk density is calculated for the <2mm fraction of the soil.

Calcium carbonate percent was calculated using the Chittick Apparatus (Dreimanis, 1962; Machette, 1986; Singer and Janitzky, 1986). Carbonate content is determined from the volume of evolved gas released through acid digestion of the sample.

RESULTS

Terrace surfaces were mapped along approximately 20 km of the Rio Salado drainage, from the confluence of the Rio Grande and the Rio Salado west to the boundary of the Sevilleta National Wildlife Preserve (Figure 12). The majority of the well-preserved surfaces were on the southern margin of the drainage, as the surfaces on the northern margin are covered in thick sheet sand deposits.

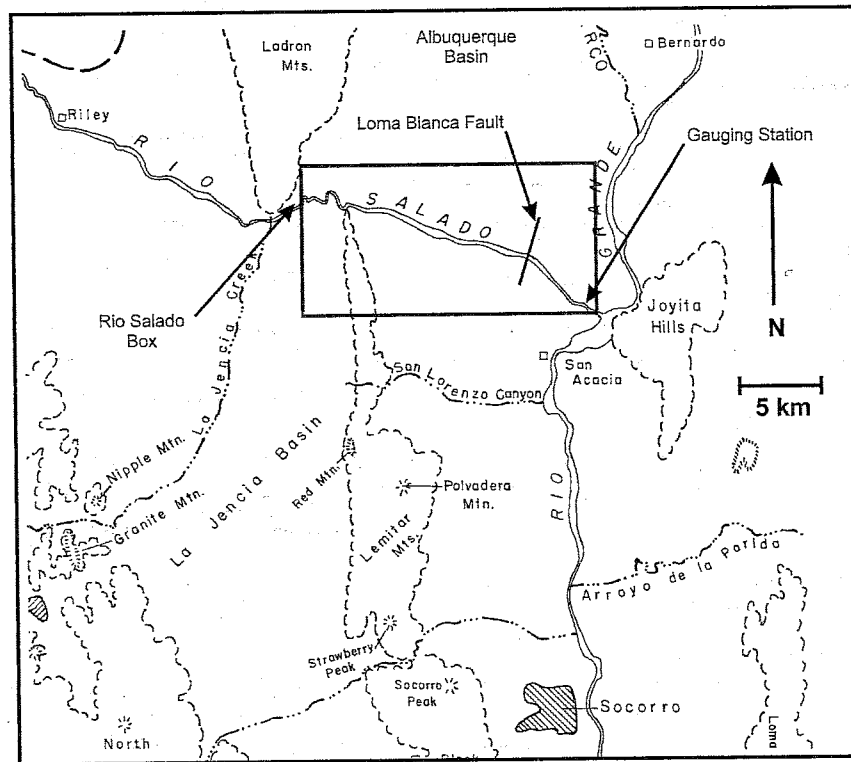


Figure 12: Extent of study area of the Rio Salado, from the Rio Grande in the east to the boundary of the Sevilleta National Wildlife preserve in the west. (Base map modified from New Mexico Geological Society, 1983).

At the scale that allows a total view of the study area, the mapped terraces are too small to distinguish. Therefore, the results are described for discrete sections of the Rio Salado (Figure 13). Each section contains a significantly large Quaternary terrace or a flight of Quaternary terraces. Additionally, sections are differentiated with respect to parent material, the local geologic map and major geologic structures affecting the drainage.

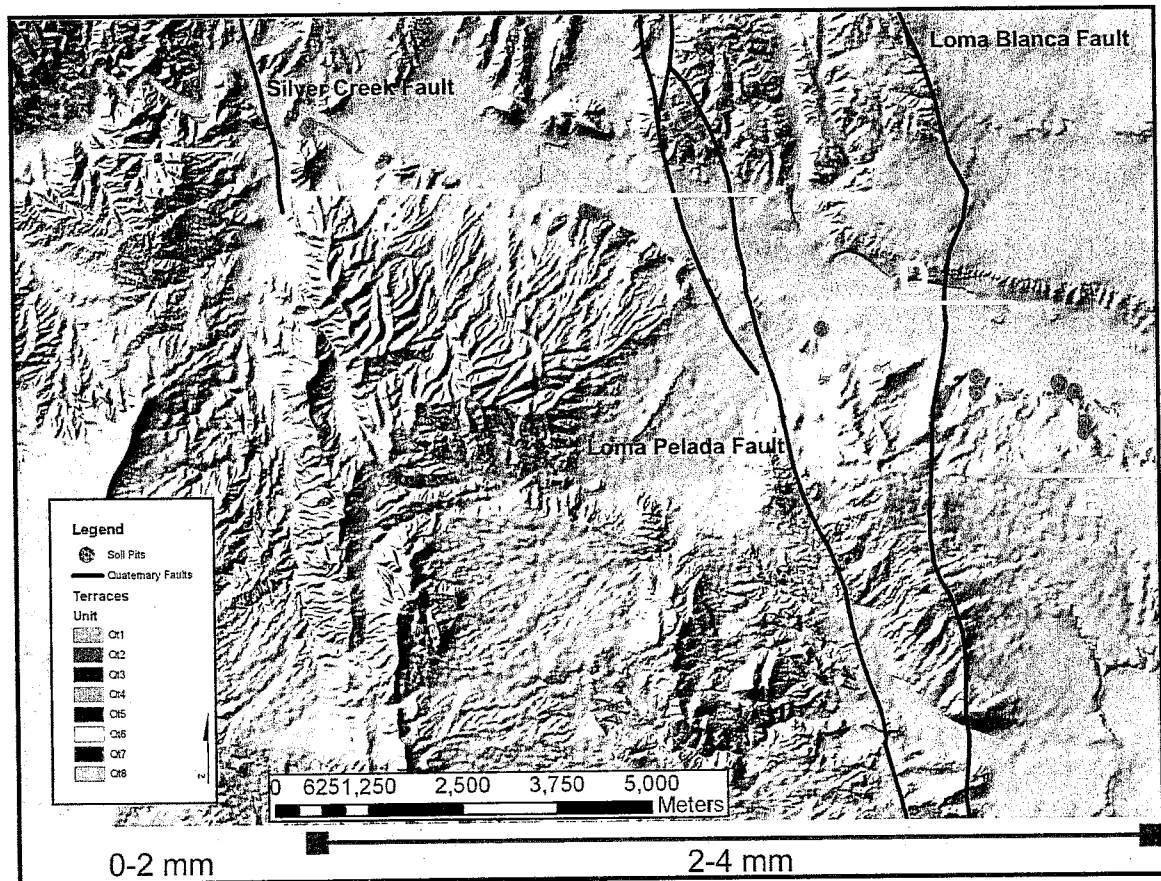


Figure 13: Study area – sections along the Rio Salado, including soil pit locations (green), mapped terraces, faults (black) and SMB uplift rates at the bottom of the image. A = Upper Reach, B = Silver Creek, C = Loma Pelada, D = Loma Blanca, E = Anticline.

Eight Quaternary terraces were identified in the study area. Complete or nearly complete flights of terraces are preserved only at the western margin of the study area and at Silver Creek. The terrace of interest, Qt6, is present in places along the channel throughout the whole study area. Qt5 is also present in all sections and Qt7 was observed in all but the Upper Reach section. These three terraces also constitute a key mapping unit, referred to as the marker sequence and were used to correlate Qt6 remnants. Soil pits were placed on terraces Qt5, Qt6 and Qt7 (Figure 13).

The Qt6 surface was the focus of the mapping exercise. As it was the best preserved terrace surface along most of the channel, Qt6 provides the most complete elevation dataset for construction of a paleochannel longitudinal profile, which in turn is compared to the modern longitudinal profile for deflection due to the magma body. Most of the Qt1 through Qt4 remnants are too small to be included in the study. Qt5, Qt6 and Qt7 are relatively well preserved in the Silver Creek section.

Terraces are differentially preserved throughout the system and terrace remnants along the Rio Salado may represent either the intact surface, a surface that has been stripped or in some intermediate condition. The same can be said for the soils formed on those surfaces. All soils were described and sampled through the C horizon (Appendix B) and the profile mass carbonate (used to approximate the age of the surface) was calculated through the B horizon (Appendix C). The profile mass carbonate was not normalized.

A total of ten soils were described in the study. The majority of the soil pits were placed on Qt6 and Qt7. Soil pits were placed on the three Qt5 terraces that had appropriate levels of surface preservation. As noted earlier, the preservation of terraces along the Rio Salado is highly variable. Most of the terrace remnants are too small and have had too much subsequent erosion to be viable locations for soil descriptions. This created a paucity of appropriate surfaces for soil sampling. To better evaluate the position of Qt6 along the channel, terrace remnants too small for soil sampling were evaluated using an auger to determine the depth to carbonate. The depth to carbonate for Qt6 was 20-35 cm below the ground surface (Appendix A). Qt7 had little or no carbonate accumulation within the upper 75 cm of the soil profile. A total of 56 auger holes were used to locate possible remnants of Qt6 to help fill in the gaps of the Qt6 longitudinal profile.

Upper Reach

The Upper Reach section extends from the western edge of the study area (the border of the Sevilleta National Wildlife Refuge) to the junction of Silver Creek (Figure 14). There is a well-preserved flight of six terraces. Additionally, Qt8 was present along the channel, downstream from this terrace flight. The terraces overlie the strongly indurated Popatosa fanglomerate bedrock. This portion of the Rio Salado is in the La Jencia basin and the channel flow seems to be perennial on the timescale of this study. This section is contained within the zone of minimum magma body uplift (0 to 2 mm of uplift per year). The channel changes direction from east-west to north-south in the upper half of the section. The average drainage gradient is 5.3 m/km over 4.6 km.

Elevations were surveyed for the six laterally continuous terraces (Table 1) (Appendix A). These surfaces directly overlie Popotosa fanglomerates and the strath of Qt6 is well exposed. Desert pavement, consisting predominantly of poorly rounded, granitic and well rounded volcanic gravels, is strongly developed on all terraces except Qt6. The Qt6 and Qt5 are preserved along the majority of the section. The higher terraces are dissected in this section.

A soil pit was located on Qt6. This surface represented the lowest terrace in the flight and was well preserved. The A horizon was thin and vesicular with 50% gravels (Appendix A). Pedogenic gypsum and salts were developed in the fine fraction at a depth of 5 – 10 cm in the B_{zy} horizon. Both the B_k and upper 20 cm of the C_k



Figure 14: Upper Reach section of the study area. One soil pit was located in this section. All six terraces preserved within this section. In addition to mapping terraces of the Rio Salado, there were two additional surfaces mapped, a Rio Grande terrace that may be related to the dissection of the Rio Salado fan and unit adjacent to the Qt7 surfaces in the lower reach of the Rio Salado.

contained illuvial clay. Carbonate development is moderate throughout the profile, peaking at 38.29% at 33 cm depth in the B_k horizon and remains relatively high into the C_k horizon (Appendix C). Profile mass CaCO₃ was 11.28 g/cm³ (Table 2).

Qt7 was not preserved in this section of the Rio Salado. The high induration of the bedrock, combined with the narrowness of the channel, contribute to increased stream power in this reach, decreasing the likelihood of preservation of weak terraces (Simcox, 1983).

Terrace	Upper Reach	Silver Creek	Loma Pelada	Loma Blanca	Anticline
Qt1	27.99	-	35.25	-	-
Qt2	26.41	-	-	-	-
Qt3	23.36	25.30	-	-	-
Qt4	16.04	18.00	-	-	-
Qt5	13.17	14.00	16.39	20.20*	32.20*
Qt6	11.66	11.80	12.63	17.20*	-
Qt7	-	10.00	10.47	10.20*	12.40*
Qt8	-	6.00	6.10	8.20*	8.50*

Table 1: Terrace elevations above the modern channel (m). * This elevation represents the minimum elevation value for the terrace surface (Insert 1).

Terrace	Upper Reach	Silver Creek	Loma Pelada	Loma Blanca	Anticline
Qt5	-	15.56	-	15.59	17.86
Qt6	11.28	13.24	12.14	-	-
Qt7	-	1.19	3.05	4.32	4.22

Table 2: Profile mass carbonate (PMC) of the Qt5, Qt6 and Qt7 terrace surfaces. PMC (g/cm³) is calculated through the B horizon and is not normalized.

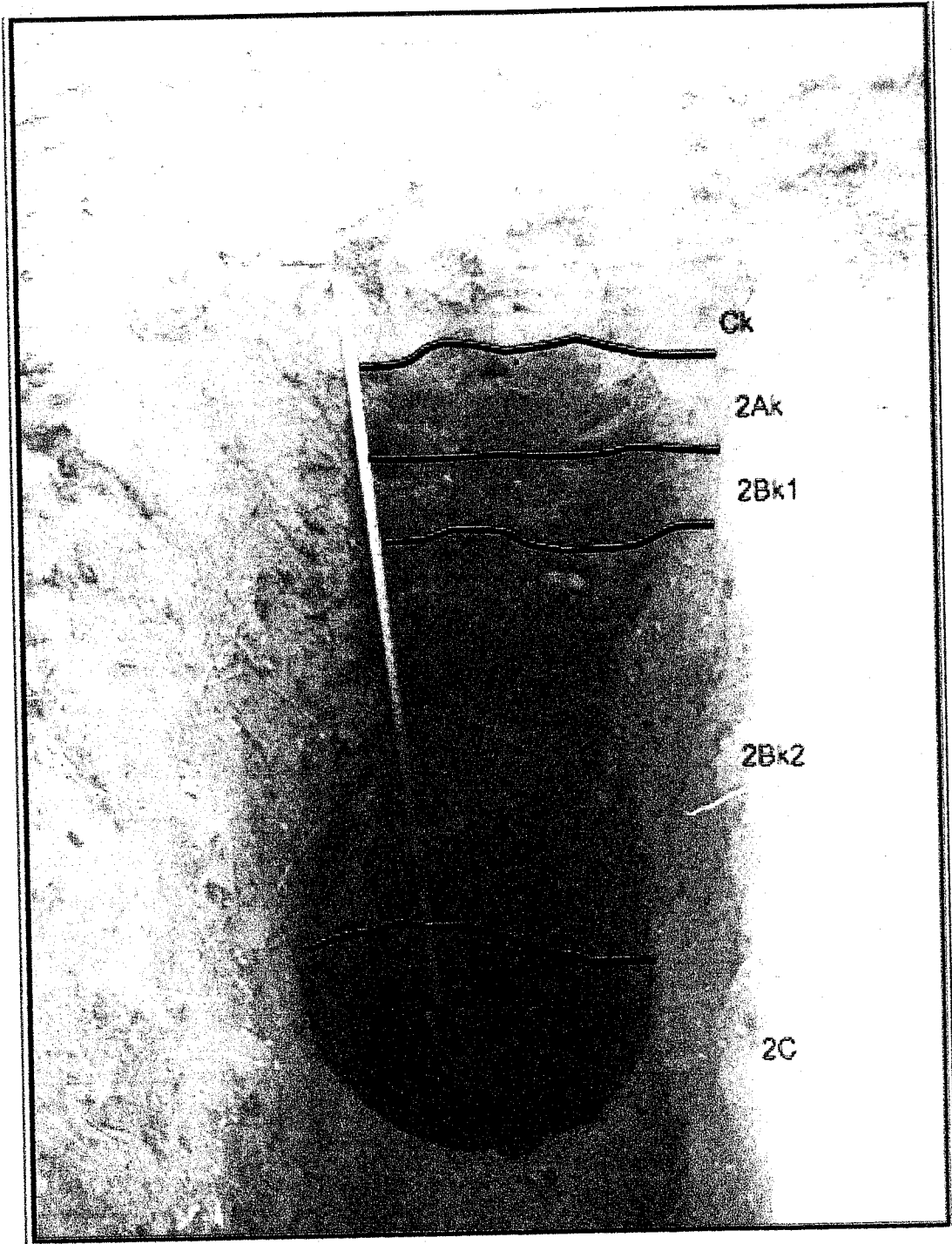


Figure 15: Qt6 soil from Silver Creek section. Sandy loam with moderate gravel content throughout profile (10-25%). Stage II carbonate.

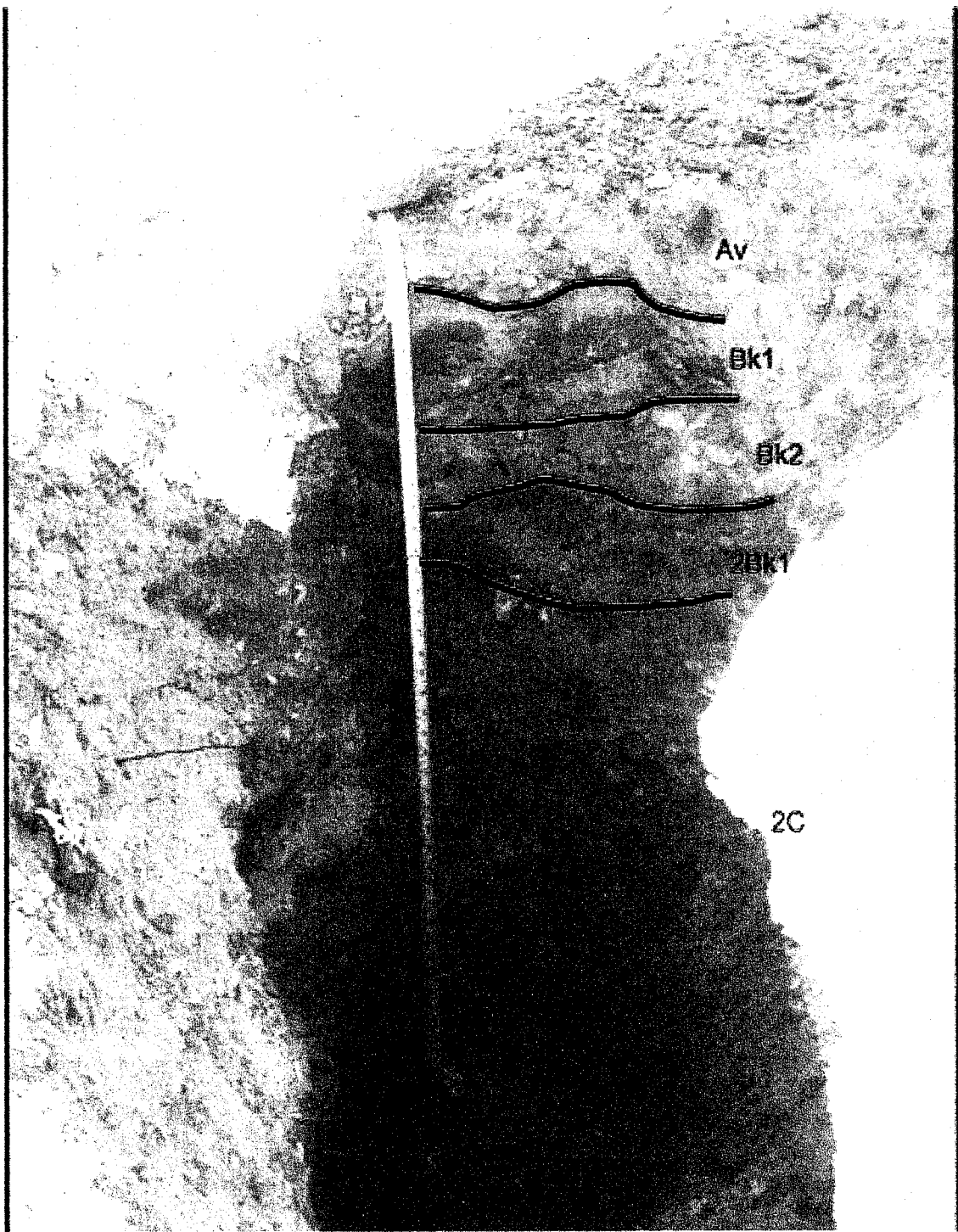


Figure 16: Qt7 soil from Loma Pelada section. Sandy loam with clean, coarse sand and small gravels at 85 cm. Stage I+ carbonate.

Five flights of terraces are preserved at the junction of the Rio Salado and the Silver Creek channel (Figure 17). At this point in the drainage, the bedrock begins to change from well-indurated fanglomerates to interbedded siltstones, fanglomerates and unconsolidated basin fill (sands and gravels). The channel also becomes much wider (probably due to the weaker nature of the bedrock). This begins the transition zone of the boundary of the magma body from minimum inflation to maximum uplift.

This is the first location downstream within the study area where Qt7 is well-preserved. Qt7 represents the lower boundary of the marker relationship. This terrace is approximately 1.8 m lower in elevation than Qt6 (Table 1). Surficially, the terraces at Silver Creek have similar vegetation and desert pavement. Soil pits were located on Qt7, Qt6 and Qt5. Qt7 contained four different stratigraphic layers. A soil formed on the top most stratigraphic unit and consisted of two thin A horizons with relatively low percentage of gravel (10%) and a weakly developed B_k horizon. The next three stratigraphic units were composed primarily of fluvial gravels with no soil development. A distinct deposit of well-sorted small gravels ranging from 2 to 10 mm was present between horizons B_{k1} and 2C_{k2}. This deposit became diagnostic for Qt7. Qt6 was 11.8 m above the channel and consisted predominantly of sand, silt and clay and was covered by a coppice dune. The Qt6 strath is clearly visible from the channel. The A horizon was relatively thick at 15 cm and contained approximately 10%

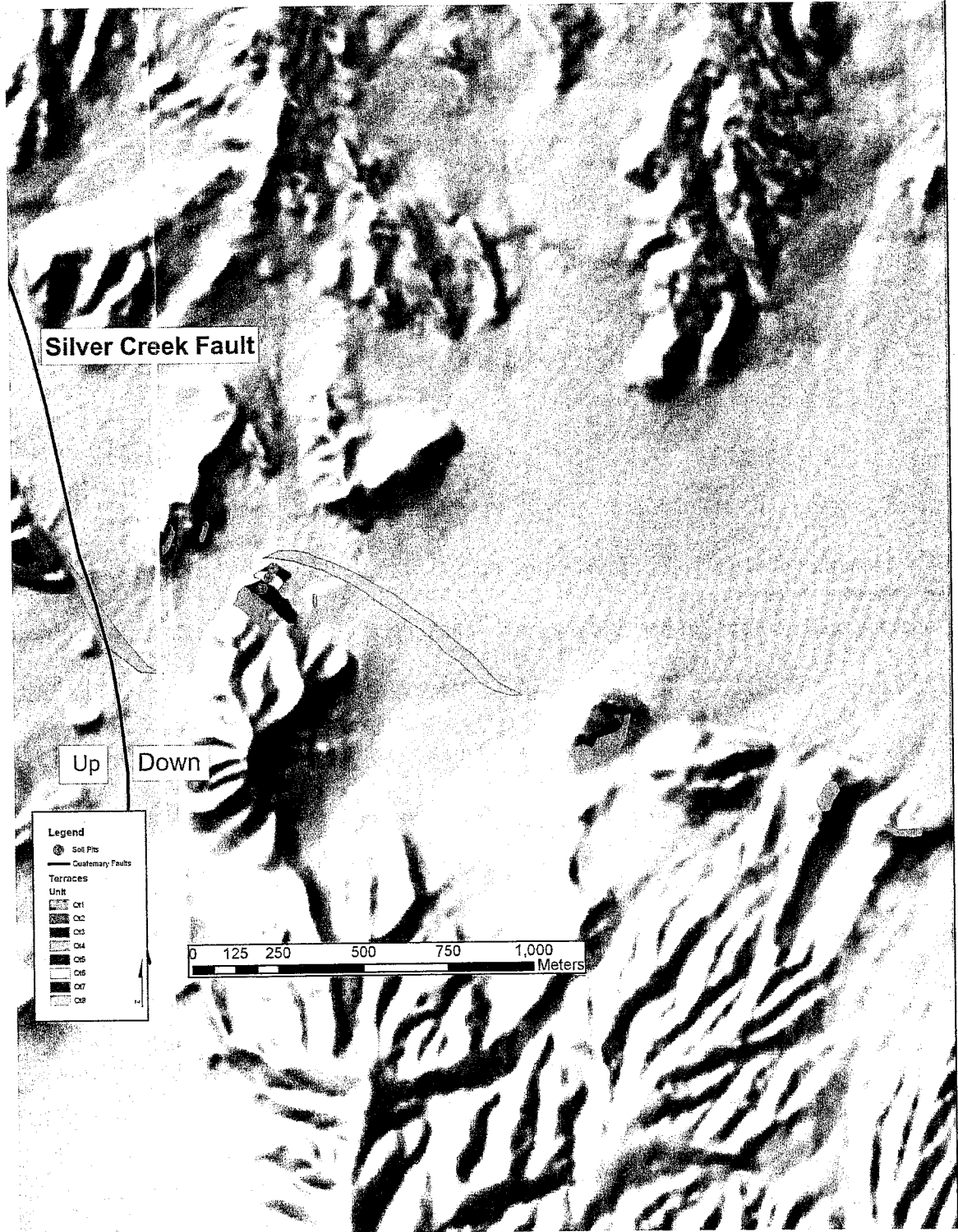


Figure 17: Silver Creek section of the study area. Three soil pits were located in this section. Five terraces preserved within this section. The fault is the Silver Creek Fault.

gravels (Figure 15). There were two B_k horizons with similar levels of well-developed carbonate. Carbonate development is moderate throughout the profile, peaking at 13.25% at 20 cm depth in the B_{kl} horizon. Carbonate content remains relatively high into the C_k horizon. Profile mass carbonate was 13.24 g/cm^3 (Table 2). Qt5 possessed a similar soil profile with the same sandy matrix. However, the profile mass CaCO_3 was higher at 15.56 g/cm^3 .

Loma Pelada

The Loma Pelada section begins east of Silver Creek, contains the Loma Pelada fault traces, and ends west of the Loma Blanca fault (Figure 18). This is the largest section within the study area and contains the least well-preserved terraces. The average drainage gradient of the Rio Salado is 6.4 m/km over 6.6 km . Two major arroyos enter the Rio Salado in this section – Canada Popatosa from the north and Valle Frutosa from the south. Terraces within this section are notably poorly preserved and are generally represented by narrow, flat-lying shelves of gravels stranded on the southern margin of the channel canyon. There are terraces within the Valle Frutosa that were not sampled as they were either much younger than the surfaces chosen for this study or they represent inset terraces of tributary drainages such as the Canada de la Tortola. This section is within the transition to maximum uplift ($2 \text{ to } 4 \text{ mm per year}$). Terraces are best preserved on top of the Popatosa fanglomerates and the Qt6 strath is visible in some of the arroyo cuts. Colluvium is deposited at the base of the terrace risers. Test pits placed

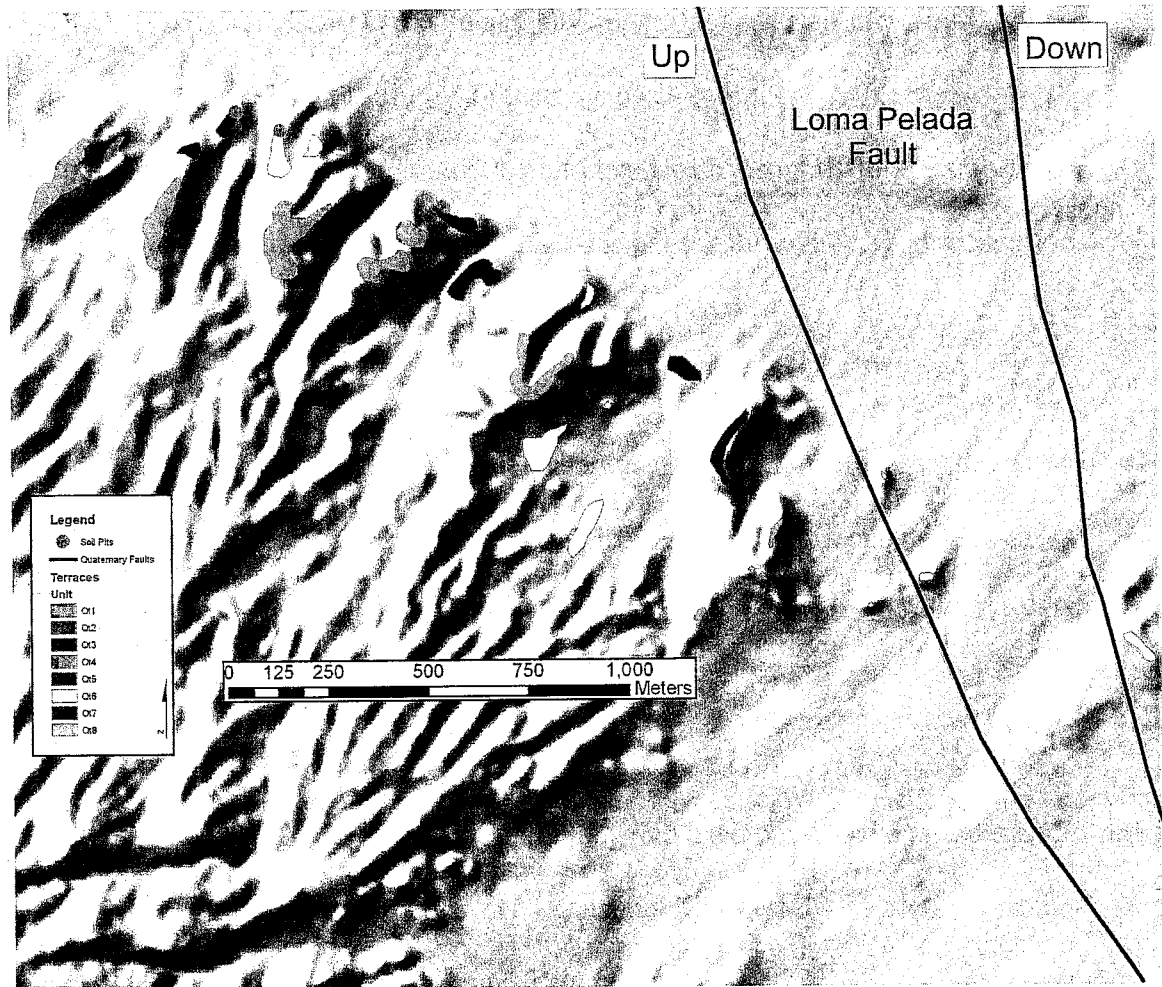


Figure 18: Loma Pelada section of the study area. Three soil pits were located in this section. Three terraces levels are preserved within this section. The faults shown are the two strands of the Loma Pelada fault.

near terrace risers confirm that the back portions of the major terraces have up to a 110 cm cover of colluvium.

Soil pits were located on Qt6 and Qt7. The Qt7 surface is elevated 10.47 meters above the active channel (Table 1). The terrace has a compositional texture of sandy loam and the lower unit ranges from sandy loam to loam with a slightly higher gravel percent (Figure 16). Carbonate development is uniformly weak throughout the profile, resulting in a profile mass total of 3.05 g/cm^3 (Table 2).

Qt6 was 12.63 m above the active channel. The compositional texture is sandier than the lower terrace. Qt6 consists of a thick loamy sand A horizon and several B_k horizons with uniform horizon carbonate percents. Profile mass CaCO_3 is 12.14 g/cm^3 .

Loma Blanca

The Loma Blanca section is 4.4 km long and encompasses the terraces east of the Loma Blanca fault (Figure 19). The active channel is widest in this section and the average drainage gradient is 5.5 m/km. This section lies within the zone of maximum uplift. Terraces are not well preserved west of the Loma Blanca fault. Stabilized dunes cover most of this area. Terraces are developed on weakly to moderately indurated Tertiary basin fill deposits. Qt7 strath gravels cut through a reddish orange overbank deposit 9 m above the active channel. There are three terrace surfaces discernable the Loma Blanca section. The Qt7 and Qt6 surfaces had a well developed desert pavement of volcanic and limestone clasts. Qt5 was covered by eolian sand deposits.

Qt7 was generally wide and laterally continuous along the Rio Salado margin. There is a thin, vesicular A horizon developed in the upper unit. Clay was present in the top two horizons to a depth of 13 cm. The maximum carbonate accumulation occurred at an average depth of 27 cm. The C horizon contained gypsum in the fine fraction. This is the only occurrence of gypsum in the soils evaluated on the Qt7 terrace and is probably a result of the proximity of this terrace to lacustrine evaporite deposits to the south. Gravel content was similar in the upper horizons. The lower stratigraphic unit was distinguishable by a large increase in gravel up to 75% by volume with an average clast diameter greater than 20 cm. Profile mass CaCO_3 was 4.32 g/cm^3 (Table 2)

Remnants of Qt6 were not suitable for soil descriptions. Auger data was used to help assess the terrace correlation for these remnants. There was a remnant of Qt5 present. Although the preservation of this surface was not ideal for a soil description, analyses revealed that the profile mass CaCO_3 was significantly higher than Qt6. This helped to further constrain the marker terrace relationship and provide an additional upper boundary for correlation.

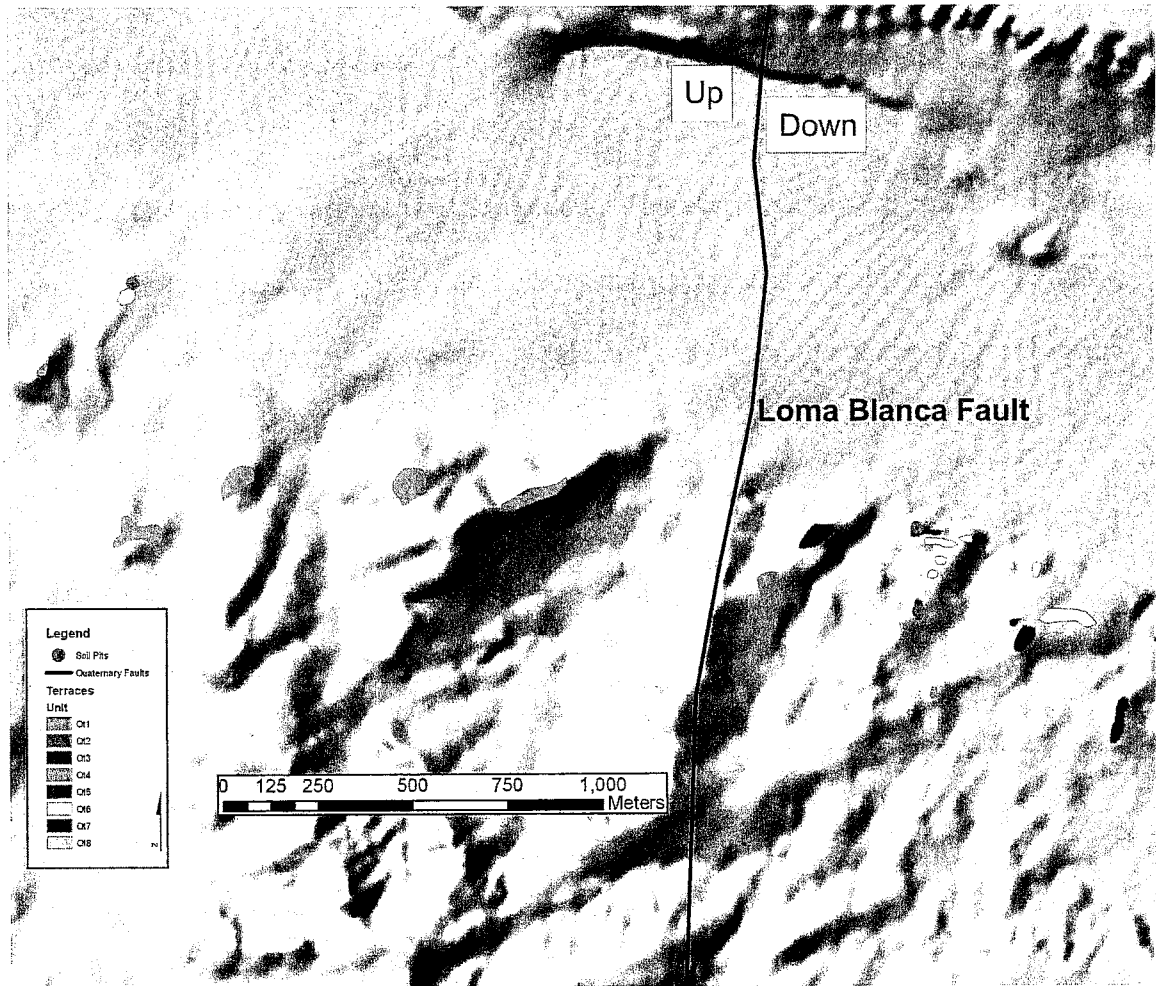


Figure 19: Loma Blanca section of the study area. Two soil pits were located in this section. Four terraces levels are preserved within this section. The fault is the Loma Blanca Fault.

Anticline

The Anticline section starts near the distinctive point that extends out into the Rio Salado at the intersection of the power line and the Sevilleta – southern Rio Salado road and ends at the scarp-like landform just west of I-25 (Figure 20). Although there is a mapped anticline in this section (Machette, 1979), noticeable offset of the terrace surface was not detected. The channel narrows to the east and much of the southern active margin has been disturbed by earthmoving equipment. The average drainage gradient is 6.0 m/km over 3.3 km. Terrace surfaces are very poorly preserved in this section. Highly eroded terrace flights are represented by thin and discontinuous layers of gravel resting on small remnants of terrace treads.

Qt7 is present at 12.4 m above the channel (Table 1). The soil developed on it contained little calcium carbonate and consists of a thin, vesicular A horizon and three B horizons. These horizons contain very little gravel. Gypsum is present in the profile beginning at a depth of 43 cm. The profile mass CaCO_3 was 4.22 g/cm^3 (Table 2).

Qt5 was 32.2 meters above the active channel and exhibited a well-developed soil. The horizons contained a significant percentage of gravels ranging from 25 to 50%. CaCO_3 development was strong throughout the profile, peaking at 54.59% at 25 cm depth in the B_k horizon. Calcium carbonate content remained relatively high into the C_k horizon. Profile mass CaCO_3 was 17.86 g/cm^3 .

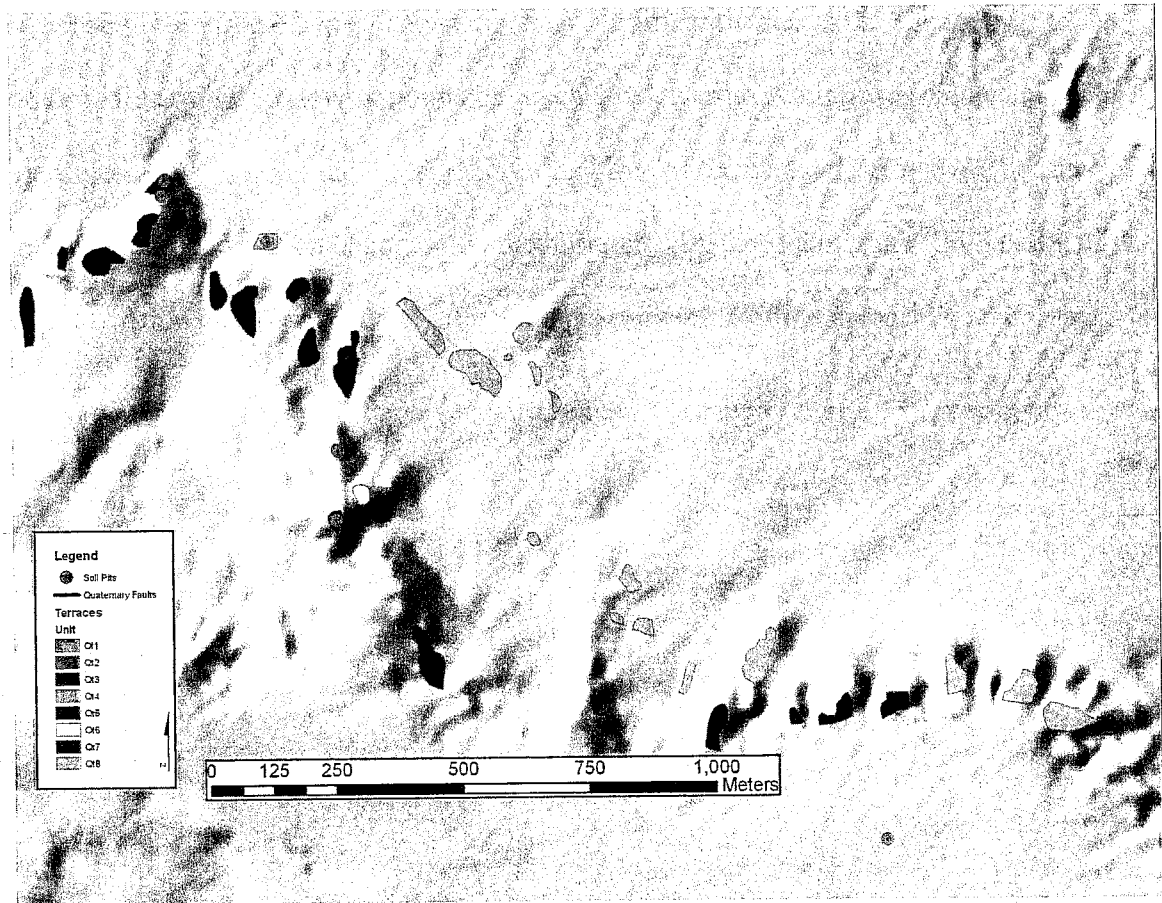


Figure 20: Anticline section of the study area. Five soil pits were located in this section. Four terraces levels are preserved within this section. The anticline is represented by a red line near the soil pit location on Qt6.

Rio Salado Longitudinal Profile

The longitudinal profile of the modern Rio Salado channel was generated using the San Acacia and Silver Creek 7.5 minute quadrangle 10 meter DEMs (Figure 21). Beginning at the furthest downstream point along the Rio Salado, elevations were extracted from the DEMs at a 500 m interval. The Rio Salado is a braided, ephemeral stream and the stream bed elevation can vary significantly across the channel width. In order to determine the lowest points in the channel, a cross section was created at each measurement point, normal to the longitudinal line of the channel. However, because of the scale of the elevation changes and the horizontal distance along the Rio Salado, this representation doesn't adequately illustrate the deflection of the paleochannel terraces.

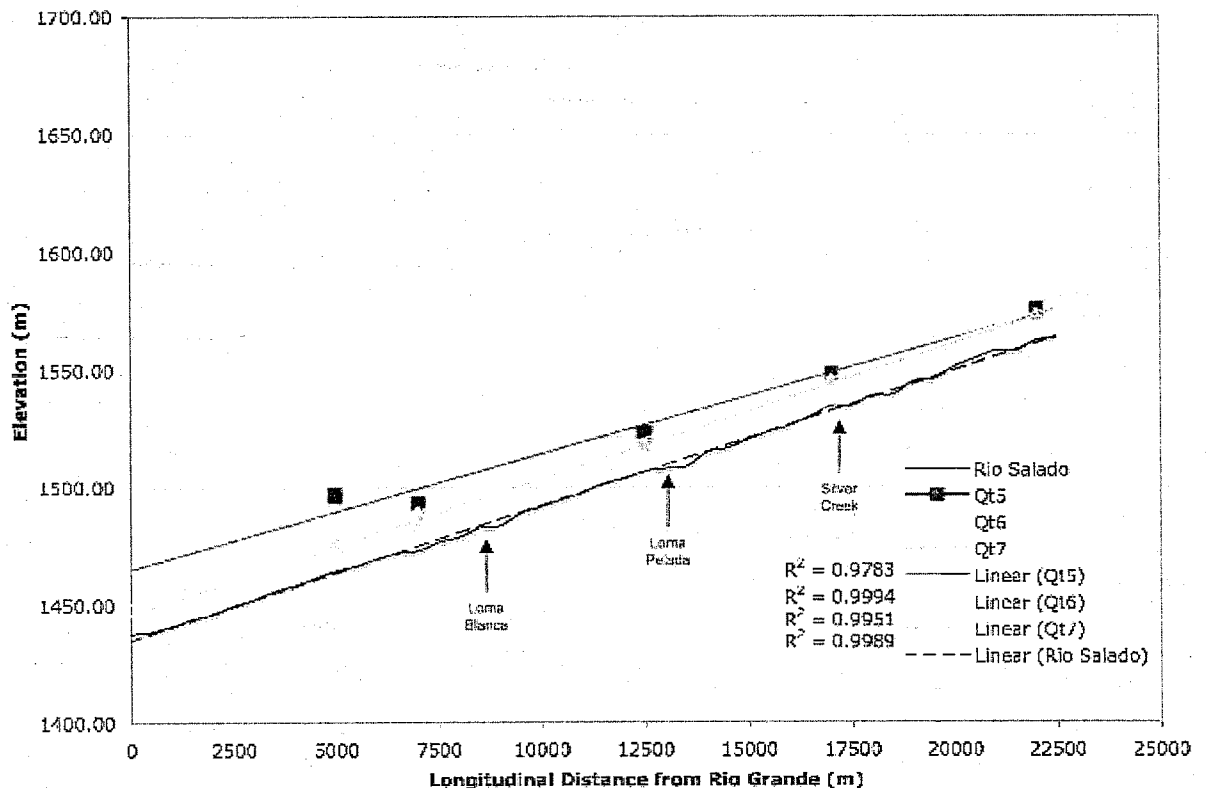


Figure 21: Longitudinal profile of the Rio Salado. The modern channel profile (blue) is essentially linear with deflections at the major faults (Loma Blanca, Loma Pelada, Silver Creek). The paleostream profile (yellow) constructed from elevations of the QT6 terraces show deflection above the modern profile.

Terrace Longitudinal Profiles

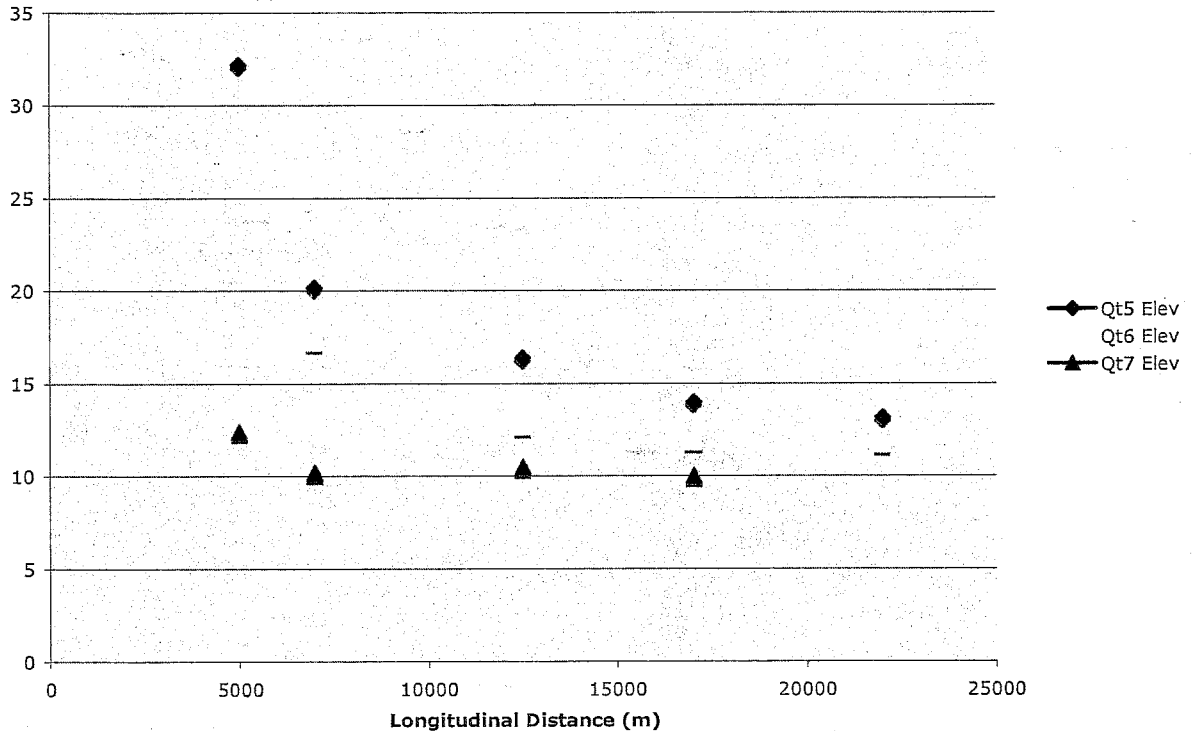


Figure 22: The pattern of deflection becomes much clearer in this graph illustrating the elevation of the terraces above the modern stream channel. The sequences of points represent the following sections: Upper Reach at 22,500 m, Silver Creek at 17,000 m, Loma Pelada at 12,500 m, Loma Blanca at 7,000 m and Anticline at 5,000 m from the confluence of the Rio Grande.

There is a distinct spatial relationship between three terraces: Qt5, Qt6 and Qt7.

Terrace Qt6 is the lowest Quaternary terrace with well-developed calcium carbonate soil horizons. Qt6 is the terrace of primary interest because it is preserved along the length of the study area. Qt7 is a weakly developed terrace that provides a lower correlative boundary for Qt6. Qt5 constrains the upper boundary for Qt6 and contains significantly more calcium carbonate in the soil profile. Remnants of this marker trio of terraces are present in most sections of the Rio Salado, although identification involved several steps.

The three surfaces were initially identified using vegetative cover. Qt6 generally had a more even distribution of creosote bushes, whereas Qt7, typically between 1.5 and 3 meters below Qt6, was covered with grasses. And Qt5 was generally 10 meters or more above Qt6, with some juniper in addition to creosote.

DISCUSSION

Stream Terrace Correlation

The discontinuity of the terrace surfaces created the need for an additional correlation factor used in the study. The relationship of the lower Quaternary surfaces Qt7, Qt6 and Qt5 was used to recognize the terrace of interest – Qt6. This marker relationship was present along the Rio Salado from its junction with Silver Creek to the downstream boundary of the study area. The marker terrace trio represents a three consecutive stream terraces with diagnostic soil carbonate content characteristics. These surface were recognized by the calcium carbonate accumulation and the strath position. If Qt6 was absent, the location of the other two marker surfaces helped maintain correlation of the terraces.

Accurate correlation of the stream terraces was crucial to this study and was complicated by the extremely poor preservation of the Quaternary terraces along the Rio Salado. However, the strath and the overlying deposits were easily discernable for the terraces formed on the well-indurated Popatosa fanglomerates, allowing for quick identification of the Qt6 surface. Although the straths were not as visible in the lower reaches of the Rio Salado, close inspection revealed these contacts in some areas.

Qt7 was not present above the junction of Silver Creek. The stream channel becomes very narrow above this point and the channel is shallowly underlain by bedrock. It is possible that the lower marker terrace has not been preserved along this stretch of the Rio Salado. Intense, monsoon rain episodes could result in sufficiently high flows to obliterate this terrace.

One obstacle to correlation was the low sampling rate, which was due to the lack of suitable surfaces sufficiently preserved for soil analysis. Even within this limited grouping of surfaces, there was still a degree of variation based upon the preservation of the individual surfaces. It is assumed that there was a period of stability following the erosion of the strath to allow for the development of a soil on that surface.

Estimated age of terraces

Two methods were used for determining age of the terraces – carbonate accumulation and uplift rate. Calcium carbonate accumulation is a characteristic of soil development in semi arid environments (Gile et al, 1966). The CaCO₃ profile mass in conjunction with CaCO₃ accumulation rates can be used to calculate the age of geomorphic surfaces (Goldstein, 2001). Calcium carbonate accumulation rates have been estimated for several locations in New Mexico, including Albuquerque, (Machette, 1985; McCalpin, 2001), Las Cruces (Gile, 1981) and Socorro Canyon (Ayarbe, 2000; Goldstein, 2001). Terrace ages in this study were calculated based the CaCO₃

accumulation rate for Socorro Canyon of $.073 \text{ g/cm}^3/\text{kyr}$. Ages were determined for surfaces Qt5, Qt6 and Qt7. As a result of the varying degree of preservation of the surfaces, age ranges are given for the three terraces. The terrace ages provide an upper limit for potential magma body uplift activity. A terrace needs to exist in order to be deflected.

The Qt7 terrace was present from the junction of Silver Creek to the eastern edge of the study area near the junction of the Rio Grande. Soil data for Qt7 was collected in the Silver Creek, Loma Pelada, Loma Blanca and Anticline sections. The profile mass carbonate ranged from 1.19 g/cm^3 to 4.32 g/cm^3 (Table 2), resulting in an age range of 16 kyr to 59 kyr for surface Qt7.

The focus terrace of this study was Qt6. The Qt6 terrace was present throughout the entire study area and soil data was collected from the Upper Reach, Silver Creek and Loma Pelada sections. Variability in profile mass carbonate ranged from 11.28 g/cm^3 to 13.24 g/cm^3 , resulting in an age range from 154 kyr to 181 kyr.

The upper terrace of the marker relation, Qt5, was sampled in three locations – Silver Creek, Loma Blanca and Anticline. The Qt5 terrace profile mass carbonate was 15.56 g/cm^3 , resulting in an age range from 213 kyr to 244 kyr.

The Qt6 surfaces have the least difference in age range, 27 kyr, which represents an 18% variation in age. Terrace age determined by profile mass carbonate is not

absolute and this variation is within the acceptable tolerances for this study. Soil evolution is a continuing process (Birkeland, 1984), some of the terraces appear to be stripped (which removes part of the soil profile) and the carbonate accumulation rate is based on an area outside the study area. Although an allowance has been made in the mass profile carbonate calculations to account for inherited carbonate, there is a variation in the amount of limestone found in the parent materials along different parts of the drainage. Additionally, some degree of variation can be attributed to soil description subjectivity and analytical errors.

Estimated duration of uplift

Rates of uplift within the areal extent of the Socorro magma body have been estimated between one to five millimeters per year (Reilinger and Oliver, 1976; Reilinger et al., 1980; Larsen and Reilinger, 1983; Ouchi, 1983; Fialko and Simons, 2001). The Fialko and Simons InSAR study (2001) provide a detailed map of the extent of the different zones of uplift. The Upper Reach section is within the area experiencing zero to two millimeters of uplift per year. The Anticline section is within the area of four millimeters of uplift per year. The modern uplift rates can be used to constrain the minimum amount of time needed to deflect the Qt6 paleochannel longitudinal profile from an undeflected state, which should be nearly parallel to the modern channel longitudinal profile.

Section	Elevation Above Channel (m)	Uplift Rate (mm/yr)							
		4.0	3.5	3.0	2.5	2.0	1.5	1.0	0.5
Anticline	-	-	-	-	-	-	-	-	-
Loma Blanca	17.20	4,300	4,914	5,733	6,880	8,600	11,467	17,200	34,400
Loma Pelada	12.63	3,158	3,609	4,210	5,052	6,315	8,420	12,630	25,260
Silver Creek	11.80	2,950	3,371	3,933	4,720	5,900	7,867	11,800	23,600
Upper Reach	11.66	2,915	3,331	3,887	4,664	5,830	7,773	11,660	23,320

Table 3: Maximum duration of uplift as determined from Qt6 elevation above modern Rio Salado channel.

An undeflected Qt6 paleochannel longitudinal profile was palinspastically reconstructed using the uplift rates for the various sections of the Rio Salado. As the endpoint of the study area in the Upper Reach section falls within the zone of no uplift, the Qt6 surface was set as a correlative, undeflected elevation between the reconstructed and actual Qt6 longitudinal profile. The altitude of the undeflected Qt6 profile was subtracted from the actual Qt6 profile. The minimum time of deflection was then calculated by determining the difference in elevations between the two Qt6 profiles and applying the InSAR uplift rates (Table 3). The maximum time of deflection was calculated using the difference between the Qt6 longitudinal profile and the modern channel multiplied by the InSAR uplift rates (Table 4).

At the maximum point of deflection for the Qt6 surface (within the Loma Blanca section) the paleochannel has been deflected by 17.2 meters. Using the maximum uplift rate of four millimeters per year, the minimum duration of uplift would be 4.3 kyr. Using the minimum uplift rate, the maximum duration of uplift would be 17.2 kyr.

An alternative case can be made to use only the difference between the Qt6 elevation in the Upper Reach section, which is presumed to be undeflected and the Qt6 elevation in the Loma Blanca section. Using this method, it would take 1.4 kyr to deflect the Loma Blanca Qt6 at the uplift rate of 4 mm per year or 11 kyr to deflect the same surface at the uplift rate of 0.5 mm per year.

Although this study discusses minimum duration of uplift, this should not be confused with minimum timing of the onset of inflation of the magma body. The rate of translation from sill inflation to disruption of the overlying strata is unknown. This problem is further complicated by the structural response, be it ductile or brittle deformation or some combination of the two end members.

There are two normal faults within the study area, Loma Blanca and Loma Pelada. Both have been classified by the USGS (2008) in the lowest slip-rate category of less than .2 mm/year, with no recurrence rate information and a most recent prehistorical deformation period of Late Quaternary (<130 ka). As the surfaces examined in this study are considerably younger than the most recent period of deformation on the faults, it is likely that the surfaces have not been offset by a large extent due to fault activity.

Section	Elevation Above Upper Reach (m)	Uplift Rate (mm/yr)							
		4.0	3.5	3.0	2.5	2.0	1.5	1.0	0.5
Anticline	-	-	-	-	-	-	-	-	-
Loma Blanca	5.54	1385.00	1,583	1,847	2,216	2,770	3,693	5,540	11,080
Loma Pelada	0.97	242.50	277	323	388	485	647	970	1,940
Silver Creek	0.14	35.00	40	47	56	70	93	140	280
Upper Reach	0.00	0.00	0	0	0	0	0	0	0

Table 4: Minimum duration of uplift of Qt6 terraces surfaces determined from adjusted Qt6 terrace altitude.

Uplift Behavior – Constant or Variable

As noted previously, there are several potential uplift behaviors for the magma body. The simplest condition is that the entire extent of the magma body behaves uniformly, the uplift rate is constant and continuous, and the overlying surface uniformly responds to the displacement caused by the inflation of the magma body. The paleoterrace longitudinal profile would exhibit a clearly linear deviation from the modern longitudinal profile. Given the variable modern uplift rates (Reilinger and Oliver, 1976; Reilinger et al., 1980; Larsen and Reilinger, 1983; Ouchi, 1983; Fialko and Simons, 2001; Newman et al., 2004), the added structural complexity of location within a rift valley and associated faulting, response to base level controlled by the Rio Grande, and differences in bedrock lithologies along the Rio Salado, it seems likely that the mechanisms of magma body uplift are complex. Several studies propose that the inflation rate could be episodic (Reilinger et al., 1980; Fialko and Simons, 2001). Once again, the surface above the magma body would reflect a linear deviation from the modern longitudinal profile. From the data collected during this study, it is not possible to

determine if the uplift of the magma body has a periodic nature. Ultimately, the resulting longitudinal profile would be similar.

The alternative magma body behavior would be variable uplift, with differing rates of inflation and deflation at different parts of the magma body. The terraces and associated soil record would be complex under these conditions. Depending upon the rate of uplift, soil formation would be weak and terraces preservation would be poor. Rapid, variable changes have been detected by two recent studies (Love et al., 2003; Newman et al., 2004). The latter study showed vertical increases on the order of 10 to 20 mm during a two year period, with no uplift recorded for a transect north of the maximum uplift zone. The study suggests that there are complexities in uplift rates due to complex sources of inflation within the magma body (Newman et al., 2004).

There is a very strong signal in support of continuous uplift (whether steady state or episodic) in the portion of the study area within the zone of maximum uplift. Presuming that the modern channel is downcutting at a rate that keeps pace with the uplift of the magma body, deflection of the surface above the magma body would create space between the uplifted terrace and the modern channel. This space would provide accommodation to form additional, intermediate terraces. Such terraces are present within the study area and their location coincides with the zone of maximum uplift (Insert A). The intermediate terraces between Qt7 and Qt6 in the Anticline section range in elevation above the channel from 15.2 meters to 24 meters. The intermediate terraces are not extensive and have weakly developed carbonate.

The Qt5, Qt6 and Qt7 paleoterrace longitudinal profiles show a linear deviation from the modern stream channel with respect to the zone of maximum uplift of the magma body. This behavior also support the model of continuous uplift over the long term inflation of the magma body. The maximum value for deflection of the Qt6 surface is on the order of 10s of kyrs. This time frame, based on deflected terrace elevations and observed uplift rates, is consistent with the estimated timing of inflation inception based on several models. Examination of tilt rates from ancestral Rio Grande in conjunction with a steady deformation rate suggests that magma body inflation began 50 kyr ago (Adams and Reilinger, 1980). Larsen et al. (1986) modeled the onset of inflation using the assumed volume of the magma body and magma flow rates calculated assuming that the volume of magma equals the volume of displaced crust. This model suggests that the magma body would have been formed on the order of 40 kyr. Fialko and Simons (2001) note that given the thickness of the magma sill (~100 m), the timing of formation cannot be on the order of 100 kyrs, as a sill of that thinness would not remain thermally viable over that length of time. This study suggests that thermal arguments support the magma body forming over a much shorter period of 100s of years.

These observations do not preclude a component of breathing behavior from the magma body occurring as well. While the overall inflation of the magma body is occurring at a steady state, there are localized areas that are experiencing large, short term rates of uplift and deflection, as noted by Love et al., (2003) and Newman et al., (2004). And while the underlying lithology is the more important control over terrace

preservation, cycling uplift and deflation episodes might contribute to the instability of the terrace surfaces.

Future work

Of course, there is a degree of error introduced into these calculations caused by several measuring factors. The first measurement factor is the elevations of the terraces above the channel. The Rio Salado is an ephemeral, braided stream and the elevation of the base of the channel is highly variable. Elevations of the terrace treads above the channel were measured fairly rudimentarily with a Jacobs staff. High precision surveying of the channel and the elevation of the terraces would provide a greater level of accuracy for the determination of uplift timing based on the uplift rate.

The second measurement factor is the relative ages of the terraces surfaces, which were determined using soil analyses, particularly calcium carbonate accumulation. A radiometric measurement of age would provide a specific age for the surfaces and allow for better correlation. There is insufficient organic matter preserved in the soils of the Rio Salado terraces for accurate ^{14}C dating. But the gravels within the terrace soils would be good candidates for cosmogenic nuclide dating.

A new study, utilizing the surfaces identified in this study, focusing on precision surveying and cosmogenic dating would refine both the correlation of the terraces and the amount of surficial uplift above the magma body.

CONCLUSIONS

It was possible to use soils to correlate the Quaternary terraces along the Rio Salado and evaluate the deflection of the terraces as an indicator of uplift of the Socorro Magma Body. The Quaternary terraces in the study area were small and discontinuous remnants. The overall poor surface preservation of the terraces lead to problems with identifying suitable surfaces for soil sampling. As many of the remnants were either stripped, actively eroding or both, careful examination of the surfaces was required in order to determine if the terrace was intact enough to provide meaningful soil data.

Three key, mostly continuous terraces were identified: Qt5, Qt6 and Qt7. All of these terraces exhibited deflection above the zone of maximum uplift of the magma body. However, the most interesting aspect of the terrace deflection pattern was the formation of additional, weakly developed terraces between Qt7 and the active flood plain. These additional strands of terraces are apparent along the southern margin of the Rio Salado in the lower reach of the drainage. There are no inset terraces between Qt5 and Qt6 or Qt6 and Qt7, leading to several possibilities. Potential inset terraces above Qt7 may not have been preserved but field reconnaissance did not reveal any inset terrace remnants between Qt5 and Qt6 or Qt6 and Qt7. The additional terraces could be a result of a sudden change in Rio Salado base level due to a tectonic event. While there may be an active fault strand

crossing this part of the Rio Salado, the drainage base level is ultimately controlled by the base level of the Rio Grande, which also flows across the zone of maximum uplift of the magma body. The potential mechanism for the formation of these inset terraces is the upward deflection of the area overlying the magma body. As the magma body inflation creates surface uplift, it creates additional room within the terrace sequence to accommodate the formation of additional surfaces as the Rio Salado erodes down through the uplifted area. With the extra terraces emplaced below Qt7, onset of inflation of the magma body could be relatively recent. While it may not be possible to definitively distinguish between constant steady surface uplift and punctuated episodes of uplift, the pattern of the additional terraces below Qt7 indicate that the most recent style of magma body inflation is fairly constant.

The age range for the Qt7 surface based on soil formation, specifically pedogenic profile mass carbonate, is between 6 and 16 kyrs. The best estimates for maximum duration of uplift of the Qt7 surface derived from the amount of deflection above the modern channel range from 3.1 kyrs with 4 mm/yr of uplift to 24.8 kyrs with an uplift rate of only 0.5 mm/yr. Clearly, the ages derived from the pedogenic characteristics is consistent with the age estimates based on uplift rates. This indicates at the least that there has been recent uplift activity, on the order of thousands to a few tens of thousands of years.

REFERENCES

Ake, J. P., and Sanford, A. R., 1988. New evidence for the existence and internal structure of a thin layer of magma at mid-crustal depths near Socorro, New Mexico, *Bulletin of the Seismological Society of America*, v. 78, no. 3, p. 1335-1359.

Bachman, G. O., and Mehnert, H. H., 1978. New K-Ar dates and the late Pliocene to Holocene geomorphic history of the central Rio Grande region, New Mexico, *Geological Society of America Bulletin*, v. 89, no. 2, p. 283-292.

Birkeland, P. W., 1984. *Soils and geomorphology*, New York, NY, Oxford University Press, 372 p.

Bull, W. B., 1990. Stream-terrace genesis: implications for soil development, in: P.L.K. Knuepfer and L.D. McFadden (Eds.), *Soils and Landscape Evolution, Geomorphology*, v. 3, p. 351-367.

Burbank, D. W., Anderson, R. S., 2001. *Tectonic geomorphology*, Berlin, Blackwell Science, 274 p.

Evans, G. C., 1963. *Geology and sedimentation along the lower Rio Salado in New Mexico*, M.S. Thesis, New Mexico Institute of Mining and Technology, 69 p.

Fialko, Y., and Simons, S., 2001. Evidence for on-going inflation of the Socorro magma body, New Mexico, from interferometric synthetic aperture radar imaging, *Geophysical Research Letters*, v. 28, no. 18, p. 3549-3552.

Goldstein, H. L., 2001. *Spatial variation in soils developed on fluvial terraces, Socorro Basin, Rio Grande Rift, central New Mexico*, M.S. Thesis, New Mexico Institute of Mining and Technology, 110 p.

Gonzales, E., 2005. Bureau of Reclamation, personal communication. *Geologic Quadrangle Map - U. S. Geological Survey*.

Hartse, H. E., and Sanford, A. R., 1992. A new map of the midcrustal Socorro magma body, *Seismological Research Letters*, v. 63, no. 1, p. 69.

Janisky, P. 1983. Enriched: Laboratory methods; particle-size analysis, Field and laboratory procedures used in a soil chronosequence study, U. S. Geological Survey Bulletin, p. 11-16.

Larsen, S., and Reilinger, R., 1983. Recent measurements of crustal deformation related to the Socorro magma body, New Mexico, in: Charles E. Chapin (Ed.), New Mexico Geological Society Thirty Fourth Annual Field Conference, Socorro Region II, p. 191-121.

Larsen, S., Reilinger, R., Brown, L. D., 1986. Evidence of ongoing crustal deformation related to magmatic activity near Socorro, New Mexico, Journal of Geophysical Research, v. 91, no. B6, p. 6283-6292.

Love, D. W., Allen, B., Chamberlin, R., Haneberg, W., 2003. First year's data from tiltmeters installed around the margins of historic uplift, centered above the Socorro magma body, Rio Grande Rift, New Mexico, New Mexico Geology, v. 25, no. 2, p. 50-51.

MacDonald, G. A., 1972. Volcanoes: Englewood Cliffs, New Jersey, Prentice-Happ, 510 p.

Machette, 1978. Geologic map of the San Acacia Quadrangle, Socorro County, New Mexico,

Newman, A. V., Chamberlin, R. M., Love, D. W., Dixon, T. H., La Femina, P. C., 2004. Rapid transient deformation from a shallow magmatic source at the Socorro magma body, NM, USA?, AGU 2004 fall meeting, Eos, Transactions, American Geophysical Union, v. 85, no. 47, Abstract G43C-02.

Ouchi, S., 1983. Effects of uplift on the Rio Grande over the Socorro magma body, New Mexico, in: Charles E. Chapin (Ed.), New Mexico Geological Society Thirty Fourth Annual Field Conference, Socorro Region II, p. 54-55.

Reilinger R., and Oliver, J., 1976. Modern uplift associated with a proposed magma body in the vicinity of Socorro, New Mexico, Geology, v. 4, no. 10, p. 583-586.

Reilinger, R., Oliver, J., Brown, L., Sanford, A., Balazs, E., 1980. New measurements of crustal doming over the Socorro magma body, New Mexico, Geology, v. 8, no. 6, p. 291-295.

Sanford, A. R., 1983. Magma bodies in the Rio Grande Rift in central New Mexico, in: Charles E. Chapin (Ed.), New Mexico Geological Society Thirty Fourth Annual Field Conference, Socorro Region II, p. 123-125.

Sanford, A. R., Jaksha, L. H., Wieder, D., 1983. Seismicity of the Socorro area of the Rio Grande Rift, in: Charles E. Chapin (Ed.), New Mexico Geological Society Thirty Fourth Annual Field Conference, Socorro Region II, p. 127-131.

Schlue, J. W., Aster, R. C., Meyer, R. P., 1996. A lower crustal extension to a midcrustal magma body in the Rio Grande Rift, New Mexico, Journal of Geophysical Research, v. 101, no. B11, p. 25,283-25,291.

Sheetz, K. E., and Schlue, J. W., 1992. Inferences for the Socorro magma body from teleseismic receiver functions, Geophysical Research Letters, v. 19, no. 18, p. 1867-1870.

Simcox, A. C., 1983. The Rio Salado at flood, in: Charles E. Chapin (Ed.), New Mexico Geological Society Thirty Fourth Annual Field Conference, Socorro Region II, p. 325 – 327.

APPENDIX A

Surveyed elevations above the active channel for terrace surfaces in the Upper Reach and Loma Pelada Sections.

Pedon	Surface	N	E	Elevation	N correction	E correction	True N	True E	True elevation
Upper Reach	Qt1	776.047	811.664	1011.948	223.953	188.336	3801504.747	309894	27.99
	Qt2	775.188	833.112	1010.369	224.812	166.888	3801503.888	309916	26.41
	Qt3	768.501	864.523	1007.319	231.499	135.477	3801497.201	309947	23.36
	Qt4	762.32	925.994	1000.003	237.68	74.006	3801491.02	310008	16.04
	Qt5	753.251	996.484	997.136	246.749	3.516	3801481.951	310079	13.17
	Qt6	663.161	991.193	995.624	336.839	8.807	3801391.861	310074	11.66
	strath	737.074	1010.251	992.55	262.926	-10.251	3801465.774	310093	8.59
	Qt6	977.992	1115.883	995.518	22.008	-115.883	3801706.692	310198	11.56
Loma Pelada	Qt5	1281.046	1018.989	1016.392	281.046	18.989	3799714.244	316700	16.39
	Qt6	1205.191	986.26	1012.625	205.191	-13.74	3799790.099	316732	12.63
	Qt7	1164.336	982.494	1010.466	164.336	-17.506	3799830.954	316736	10.47
	Qt8	1155.168	1083.719	1006.1	155.168	83.719	3799840.122	316635	6.10

APPENDIX B

Soil Descriptions

PEDON	HORIZON	DEPTH (cm)	THICKNESS (cm)	% GRAVEL	% SAND	% SILT	% CLAY	TEXTUR E (lab)	BULK DENSITY	% CaCO3
Anticline Qt5	A	0-10	10	25	58	22	20	SCL	1.42	34.02
	Bk	10-25	15	50	63	21	17	SL	1.51	61.77
	Bk	25-46	21	50	70	14	16	SL	1.61	59.31
	C	46-55	9	10	79	10	11	SL	1.61	47.50
	C	55-70	25	10	84	9	7	LS	1.56	39.00
	C	70-78	8	10	83	10	7	LS	1.66	44.50
Anticline Qt7	Av	0-5	5	0	50	34	15	L	1.58	11.04
	Bk1	5-23	18	0	70	18	12	SL	1.58	18.01
	Bk2	23-43	20	5	66	NA	NA	SL	1.39	10.02
	Bk2	@43	1	5	74	25	0	LS	1.42	11.42
	Bykw	43-60	17	10	96	4	0	S	1.65	7.51
	Cy	60-90	30	75	90	7	3	S	1.65	5.12
	Cy	90-120	30	75	95	4	1	S	1.65	7.76
Loma Blanca Qt7	Av	0-5	5	30	57	31	12	SL	1.53	4.35
	Bk1	5-13	8	25	64	22	14	SL	1.33	19.39
	Bk2	13-42	29	75	89	8	4	S	1.65	36.45
	Cy	42-68	26	30	98	2	1	S	1.65	18.40
	2C	68-140	72	75	90	6	4	S	1.60	25.81
Loma Pelada Qt6	A	0-19	19	5	78	15	7	LS	1.56	14.50
	Bk1	19-54	35	10	72	20	8	SL	1.57	16.18
	Bk2	54-77	23	20	86	9	5	LS	1.55	15.02
	Bk3	77-110	33	20	84	11	6	LS	1.53	15.57
	2C	110-180	70	75	93	5	2	S	1.65	33.56
Loma Pelada Qt7	Av	0-5	5	5	68	22	10	SL	1.56	10.25
	Bk1	5-38	33	5	67	21	12	SL	1.56	10.18
	Bk2	38-51	13	10	70	20	10	SL	1.57	10.66
	2Bk1	51-76	25	20	47	35	18	L	1.41	9.72
	2Bk2	76-96	20	20	55	30	16	SL	1.43	11.47
	2Bk2	96-116	20	20	59	27	14	SL	1.35	11.50
	2Bk2	116-136	20	20	67	20	12	SL	1.46	12.87
	2Bk2	136-168	32	20	49	34	17	L	1.27	14.05
Upper Reach Qt6	Av	0-5	5	50	57	27	16	SL	1.43	14.22
	Bzy	5-10	5	20	54	40	7	SL	1.30	33.23
	Btk	10-33	23	10	50	24	26	SCL	1.22	45.47
	Ctk	33-50	17	15	58	21	21	SCL	1.49	42.92
	Ck	50-65	15	15	63	19	18	SL	1.69	36.59
	Ck	65-85	20	15	70	16	15	SL	1.73	28.56

PEDON	HORIZON	DEPTH (cm)	COLOR (m)	COLOR (d)	% GRAVEL	NSISTENCE (m)	NSISTENCE (d)	TEXTURE
Anticline Qt5	A	0-10	7.5 YR 5/3	7.5 YR 6/4	25	ss/sp	so	SL
	Bk	10-46	7.5 YR 6/4	7.5 YR 7/2	50	so/po	h	SL
	C	46-78	7.5 YR 5/4	7.5 YR 6/3	10	so/po	sh	SL
Anticline Qt7	Av	0-5	7.5 YR 5/4	7.5 YR 6/4	0	s/ps	sh	SL
	Bk1	5-23	7.5 YR 3/4	7.5 YR 5/4	0	s/p	sh	SL
	Bk2	23-43	10 YR 3/4	10 YR 5/3	5	ss/po	lo	LS
	Bykw	43-60	10 YR 3/4	10 YR 6/3	10	so/po	lo	LS
	Cy	60-120	5 YR 4/3	2.5 YR 6/3	75			S
Loma Blanca Qt7	Av	0-5	10 YR 4/3	10 YR 5/4	30	ss/po	so	SL
	Bk	5-13	10 YR 4/3	10 YR 5/4	25	so/po	so	SL
	Bk	13-42	7.5 YR 4/3	5 YR 7/2	75	so/po	so	SL
	Cy	42-68	10 YR 5/3	10 YR 7/2	30			S
	2C	68-140	7.5 YR 5/3	7.5 YR 7/3	75			S
Loma Pelada Qt6	Av	0-19	7.5 YR 5/4	7.5 YR 6/4	5	ss/po	so	SL
	Bk1	19-54	7.5 YR 4/4	7.5 YR 5/4	10	so/po	sh	SL
	Bk2	54-77	7.5 YR 4/3	7.5 YR 6/3	20	so/po	sh	SL
	Bk3	77-110	7.5 YR 5/4	7.5 YR 7/4	20	so/po	sh	SL
	Ck	110-180	7.5 YR 5/4	7.5 YR 6/3	75			S
Loma Pelada Qt7	Av	0-5	7.5 YR 5/4	7.5 YR 6/4	5	ss/po	so	SL
	Bk1	5-38	7.5 YR 3/4	7.5 YR 5/4	5	so/po	sh	LS
	Bk2	38-51	7.5 YR 4/3	7.5 YR 5/4	10	so/po	sh	LS
	2Bk1	51-76	7.5 YR 6/4	7.5 YR 6/3	20	so/po	sh	LS
	2Ck	76-168	7.5 YR 5/6	7.5 YR 6/4	20			S
Silver Creek Qt5	A	0-3			20	ss/po	so	SL
	Bk1	3-20			25	so/po	sh	LS
	Bk2	20-42			25	so/po	sh	LS
	Bk3	42-67			25	so/po	sh	LS
	Bk4	67-83			30	so/po	sh	LS
	Ck	81-101			25	so/po	so	S
Silver Creek Qt6	Ck	0-12			10	so/po	so	S
	2Ak	12-27			20	ss/po	sh	SL
	2Bk1	27-39			25	so/po	sh	LS
	2Bk2	39-110			25	so/po	sh	LS
	2C	110-120			5	so/po	so	S
Silver Creek Qt7	Ak	0-2			20	so/po	so	LS
	Ak2	2-4			20	so/po	so	LS
	Bk1	4-15			25	so/po	so	S
	2Ck2	15-19			25	so/po	so	S
	3Ck3	19-29			25	so/po	so	S
	4Ck4	29-39			25	so/po	so	S
Upper Reach Qt6	Av	0-5	7.5 YR 5/4	7.5 YR 7/4	50	ss/ps	so	SL
	Bzy	5-10	7.5 YR 5/4	7.5 YR 6/4	20	ss/ps	so	SL
	Bk	10-33	7.5 YR 5/4	7.5 YR 7/4	10	ss/ps	sh	SL
	Ck	33-85	7.5 YR 5/6	7.5 YR 6/4	15	so/po	so	SL

APPENDIX C

Profile Mass Carbonate calculations

BDF = Bulk Density Fraction

CF = Carbonate Fraction

G = Gravel

PMC = Profile Mass Carbonate

PEDON	HORIZON	DEPTH (cm)	T	BDF	%CF	%G	PMC	PMC thru B
Anticline Qt5	A	0-10	10	1.423677364	26.83962606	25	2.865822606	2.865822606
	Bk	10-25	15	1.51	54.59359786	50	6.182724957	6.182724957
	Bk	25-46	21	1.61	52.13281999	50	8.81305322	8.81305322
	Ck	46-55	9	1.61	40.3203722	10	5.258179738	0
	Ck	55-70	15	1.56	31.82373183	10	6.702077924	0
	Ck	70-78	8	1.66	37.31978104	10	4.46046023	0
								17.86160078
Anticline Qt7	Av	0-5	5	1.577553308	3.85812364	0	0.304319785	0.304319785
	Bk1	5-23	18	1.58	10.82896576	0	3.079757862	3.079757862
	Bk2	23-43	20	1.39	2.844283093	5	0.751175165	0.751175165
	Bk2	@43	0	1.42	4.240454225	5	0	0
	Bykw	43-60	17	1.65	0.33414325	10	0.084354463	0.084354463
	Cy	60-90	30	1.65	-2.059320035	75	-0.254840854	0
	Cy	90-120	30	1.65	0.575794807	75	0.071254607	0
								4.219607276
Loma Blanca Qt7	Av	0-5	5	1.527669281	-2.826384058	30	-0.151122304	-0.151122304
	Bt	5-13	8	1.33	12.21107923	25	0.974444123	0.974444123
	Bk	13-42	29	1.65	29.26548711	75	3.500883896	3.500883896
	Cy	42-68	26	1.65	11.22312549	30	3.370304585	0
	2C	68-140	72	1.6	18.63408856	75	5.366617505	0
							4.324205715	
Loma Pelada Qt6	Av	0-19	19	1.558692688	7.321973412	5	2.059993509	2.059993509
	Bk1	19-54	35	1.57	8.99747201	10	4.449699783	4.449699783
	Bk2	54-77	23	1.55	7.840650817	20	2.236153613	2.236153613
	Bk3	77-110	33	1.53	8.392653905	20	3.389960765	3.389960765
	Ck	110-180	70	1.65	26.38467798	75	7.618575765	0
							12.13580767	
Loma Pelada Qt7	Av	0-5	5	1.56	3.07	5	0.227487	0.227487
	Bk1	5-38	33	1.56	3.000505914	5	1.467427422	1.467427422
	Bk2	38-51	13	1.57	3.48178334	10	0.639568782	0.639568782
	2Bk1	51-76	25	1.41	2.543873856	20	0.717372427	0.717372427
	2Ck	76-96	20	1.43	4.290381853	20	0.981639368	0
	2Ck	96-116	20	1.35	4.32019289	20	0.933161664	0
	2Ck	116-136	20	1.46	5.686959645	20	1.328473773	0
	2Ck	136-168	32	1.27	6.872337332	20	2.234334313	0
							3.051855631	
Silver Creek Qt5	A	0-3	3	1.24	15.04996769	20	0.447887039	0.447887039
	Bk1	3-20	17	1.61	23.1860463	25	4.759515653	4.759515653
	Bk2	20-42	22	1.7	20.75919988	25	5.822955567	5.822955567
	Bk3	42-67	25	1.69	0.506003664	25	0.160339911	0.160339911
	Bk4	67-83	16	1.7	22.95791794	30	4.371187575	4.371187575
	Ck	81-101	20	1.73	42.04218701	25	0	0
							15.56188574	
Silver Creek Qt6	Ck	0-12	12	1.35	9.949952039	10	1.450703007	1.450703007
SC-2	2Ak	12-27	15	1.55	13.25092431	20	2.464671922	2.464671922
SC-2	2Bk1	27-39	12	1.55	7.449943636	25	1.039267137	1.039267137
SC-2	2Bk2	29-110	81	1.55	8.8	25	8.2863	8.2863
SC-2	2C	110-120	20	1.55	-4.13	5	0	0
								13.24094207

Silver Creek Qt7	Ak	0-2	2	1.33	3.485374303	20	0.074168765	0.074168765
	Ak2	2-4	2	1.35	6.882989676	20	0.148672577	0.148672577
	Bk1	4-15	11	1.47	7.947933853	25	0.963885678	0.963885678
	2Ck2	15-19	4	1.63	6.120439629	25	0.299289498	0
	3Ck3	19-29	10	1.59	4.82710234	25	0.575631954	0
	4Ck4	29-39	10	1.63	0.002578873	25	0.000315267	0
								1.18672702
Upper Reach Qt6	Av	0-5	5	1.4337225	7.039843806	50	0.252329562	0.252329562
	Bzy	5-10	5	1.3	26.04599328	20	1.35439165	1.35439165
	Bk	10-33	23	1.22	38.29142809	10	9.670117251	9.670117251
	Ck	33-50	17	1.49	35.73628794	15	7.694201474	0
	Ck	50-65	15	1.69	29.41361831	15	6.337899405	0
	Ck	65-85	20	1.73	21.37850683	15	6.287418858	0
								11.27683846